1 **Short Title:** NIP2;1 lactic acid efflux during low oxygen stress

2 *Author to whom correspondence should be sent: Daniel M. Roberts, e-mail: drobert2@utk.edu

3 BCMB Dept., The University of Tennessee, Knoxville, TN, USA Phone: 1-865-974-4070, Fax:
4 1-865-974-6306,

5

The *Arabidopsis thaliana* NIP2;1 Lactic Acid Channel promotes Plant Survival Under Low Oxygen Stress

Zachary Beamer[1], Pratyush Routray[1,3*], Won-Gyu Choi[2], Margaret K. Spangler[1], Ansul Lokdarshi[1], and Daniel M. Roberts[1*]

[1]Department of Biochemistry and Cellular, and Molecular Biology, the University of Tennessee, Knoxville, TN 37996; [2]Department of Biochemistry and Molecular Biology, The University of Nevada, Reno, NV 89557.

[3]Present address: Boyce Thompson Institute, Ithaca, New York 14853, USA.

One-sentence Summary: The NIP2;1 lactic acid permease is necessary for an optimum response to low oxygen stress through the release of lactate from roots during hypoxia stress.

Author Contributions **Z.B.,** organized and executed the majority of the experiments, and together with P.R. wrote the manuscript; **P.R.**, co-corresponding senior author who directed in the design and supervision of the experiments, generated the complementation lines, conducted experiments on phenotype and was involved in analysing the data and organizing the manuscript; **W.G.C.,** initiated the early work, generated and characterized the promoter-GUS lines, and performed early analyses of the *nip2;1* T-DNA line; **M.S.,** undergraduate research student who assisted in phenotype survival analyses; **A.L.**, assisted in localization experiments as well as the QY_{max} measurements; **D.M.R**., supervisor of the project, obtained funding for the work, and was involved in the design of experiments, analysis and interpretation of the data, and co-edited the manuscript with PR. DMR agrees to serve as the contact, communication, and source for materials emerging from this project.

Funding Information: This work was supported by National Science Foundation Grant MCB-1121465 to DMR.

*Corresponding authors email drobert2@utk.edu, and pr474@cornell.edu .

Abstract

Under anaerobic stress *Arabidopsis thaliana* induces the expression of a collection of core hypoxia genes that encode proteins associated with an adaptive response. Included in these core hypoxia genes is *NIP2;1*, which encodes a member of the "Nodulin-like Intrinsic Protein" (NIP) subgroup of the aquaporin superfamily of membrane channel proteins. Under normal growth, *NIP2;1* expression is limited to the "anoxia core" region of the root stele, but shows substantial induction in response to low oxygen stress (as high as 1000-fold by 2-4 hr of hypoxia challenge), and accumulates in all root tissues. During hypoxia, *NIP2;1-GFP*, accumulates on the cell surface by 2 hr and then is distributed between the cell surface and internal membranes during sustained hypoxia, and remains elevated in root tissues through 4 hrs of reoxygenation recovery. T-DNA insertional mutant *nip2;1* plants show elevation of lactic acid within root tissues, and a reduced efflux of lactic acid and acidification of the external medium. Together with previous biochemical evidence demonstrating that NIP2;1 has lactic acid permease activity, the present work supports the hypothesis that the protein facilitates the release of cellular lactate to the rhizosphere to prevent lactic acid toxicity. In support of this, *nip2;1* plants show poorer survival to argon-induced hypoxia stress. *Nip2;1* mutant plants also show elevated expression of ethanolic fermentation transcripts, as well as reduced expression the lactate metabolic enzyme GOX3, suggesting that the altered efflux of lactate through NIP2;1 regulates other pyruvate and lactate metabolism pathways.

Introduction

As obligate aerobes, land plants require a continuous supply of oxygen to support energy demand. Oxygen deprivation stress from flooding or poor soil aeration depresses cellular respiration leading to an energy crisis that triggers a variety of genetic, metabolic, and developmental adaptation strategies (Voesenek and Bailey-Serres, 2013, 2015). In Arabidopsis, low oxygen stress triggers the preferential transcription and translation of a collection of "core" hypoxia-induced genes that encode glycolytic/fermentation enzymes, other metabolic proteins, and various signal transduction proteins and transcription factors involved in the adaptive response (Mustroph et al., 2009; Mustroph et al., 2010). Among the hypoxia-induced core response transcripts is an aquaporin-like membrane channel protein, Nodulin Intrinsic Protein 2;1 (Choi and Roberts, 2007).

Nodulin 26-like" Intrinsic Proteins (NIPs) are a terrestrial plant-specific subfamily of the aquaporin-superfamily that show structural and functional homology to the soybean root nodule-specific protein nodulin 26 (Roberts and Routray, 2017). NIPs possess the canonical aquaporin "hourglass" fold, but have diverged as multifunctional transporters of a wide variety of substrates including glycerol, ammonia, and a variety of essential as well as boric acid, silicic acid, and toxic metalloid hydroxides (Roberts and Routray, 2017; Pommerrenig et al., 2020). Based on structural modelling, NIPs can be segregated into three "pore families" that have conserved amino acids within their aromatic-arginine (ar/R) selectivity filters (Roberts and Routray, 2017). NIP2;1, along with NIP1;1, NIP1;2, NIP3;1, NIP4;1 and NIP4;2, belongs to the Arabidopsis NIP I subgroup (Johanson et al., 2001; Routray and Roberts, 2017). NIP I proteins have an ar/R amino acid composition similar to nodulin 26 (Wallace and Roberts, 2004), and show a transport selectivity for water, glycerol, and ammonia as natural substrates (Roberts and Routray, 2017), as well as the ability to be permeated by toxic metalloids (e.g., arsenite and antimonite) (Kamiya and Fujiwara, 2009; Kamiya et al., 2009; Xu et al., 2015). Biochemical analysis of NIP2;1 in Xenopus oocytes showed that it lacks the typical NIP I transport properties and is impermeable

to classical NIP substrates (Choi and Roberts, 2007). Instead, NIP2;1 shows pH-dependent transport of lactic acid (Choi and Roberts, 2007).

Lactic acid is the end product of lactate fermentation, one the fermentative pathways employed by plants to sustain energy production under oxygen limiting conditions and other stress conditions in which respiration is repressed (Drew, 1997; Gibbs and Greenway, 2003). Accumulation of lactic acid increases the acid load in the cytosol, and is among the factors that contribute to the cellular acidification observed during low oxygen stress (Davies et al., 1974; Roberts et al., 1984; Felle, 2005). Hypoxia-induced fermentation is accompanied by the acquisition of the ability of plant roots to efflux lactic acid to the rhizosphere (Xia and Saglio, 1992; Rivoal and Hanson, 1993; Xia and Roberts, 1994; Dolferus et al., 2008). In maize root tips, this lactic acid efflux mechanism is correlated with reduced susceptibility to low oxygen stress from acclimation, it is proposed to be an adaptive mechanism to reduce cytosolic acidification or other toxic effects of cellular lactic acid/lactate accumulation (Xia and Saglio, 1992; Xia and Roberts, 1994).

The previous finding that NIP2;1 is selectively permeable to lactic acid upon expression in oocytes, together with its identification as a core-hypoxia gene product, has led to the hypothesis that it mediates the efflux and/or compartmentation of lactic acid during the Arabidopsis response to low oxygen stress (Choi and Roberts, 2007). However, this has yet to be investigated in planta. The objective of this research was to test this hypothetical function of NIP2;1 during the Arabidopsis hypoxia response. In this study, it shown that a T-DNA insertional *nip2;1* mutant exhibits poor tolerance of low oxygen stress compared to wild-type. Further, it is shown that the efflux of lactate from hypoxia-stressed roots to the media from the roots requires NIP2;1 expression. NIP2;1 localization was observed to vary between internal membranes and the plasma membrane during the course of hypoxia and recovery, consistent with previous observations suggesting dual localization of the protein. Lastly, evidence is presented that the transcripts encoding fermentation and pyruvate/alanine metabolism enzymes are altered in

nip2;1 mutant plants compared to wild-type plants. Overall, the data support a role for NIP2;1 as a lactic acid efflux channel, and suggest that this activity could help control the expression of enzymes that metabolize pyruvate during the Arabidopsis hypoxia response.

Results

***NIP2;1* expression is induced early during hypoxia primarily in root tissue** Hypoxia treatment of two week old Arabidopsis seedlings resulted in a rapid increase in *NIP2;1* expression in root tissues with Q-PCR analysis revealing a >1000-fold increase in *NIP2;1* transcript levels within two hours after the onset of anaerobiosis (Fig. 1A). *NIP2;1* transcript levels then showed a sharp decline by 12 hr but still remained over 100-fold elevated relative to normoxic controls before leveling off at 24 hr (Fig. 1A). While *NIP2;1* is predominantly a root transcript, hypoxia also induced *NIP2;1* expression in shoot tissues, but with a lower overall expression (40-fold relative to basal levels) compared to roots (Fig. 1A inset). In addition, the time course of accumulation in shoots was delayed when compared to root tissues and expression did not peak until 12 hr treatment.

Similar patterns of *AtNIP2;1* expression were observed with two week old *AtNIP2;1* *promoter::GUS* fusion plants subjected to the same oxygen deprivation regime (Fig 1B). Analysis of the cellular localization of GUS staining under normoxic conditions showed that expression is principally limited to roots with little staining detected in shoot tissues (Fig. 1B). Cross-sections of unstressed (normoxic) roots showed that GUS staining was principally observed in the cells of the stele (pericycle, phloem and procambium,) with little or no GUS signal apparent in endodermal, cortical and epidermal cells (Supplemental Fig. 1, Fig. 1B). At 4 hr after the induction of hypoxia, root tissues showed an increase in intensity of the GUS staining in the stele as well as the appearance of the GUS signal in the cortex, epidermis and root hairs (Fig. 1B). Similar to the Q-PCR result, this staining peaked at 4 hr post hypoxic treatment and then decreased by 12 hr post treatment (Fig. 1B), although the expression at these later time points was still much higher than the basal expression in the unstressed roots

(Fig. 1B). In comparison to roots, increases in GUS expression in shoots were less acute and appeared more slowly and the expression was mainly restricted to the vascular tissues of leaves (Fig. 1C).

***NIP2;1* enhances plant survival under low oxygen conditions** Core hypoxia-response gene loss-of-function mutants generally result in reduced survival or increased sensitivity to low oxygen stress (Ismond et al., 2003; Kursteiner et al., 2003; Licausi et al., 2010; Giuntoli et al., 2014; Sorenson and Bailey-Serres, 2014; Lokdarshi et al., 2016). To investigate whether *NIP2;1* is necessary for hypoxia stress survival, a T-DNA insertion mutant (WiscDsLox233237_22K; referred to here as *nip2;1)* line was studied. The *nip2;1* line contains a T-DNA insertion within the promoter region (-30) between a cluster of Anaerobic Response Elements and the transcriptional start site (Fig. 2A). Consistent with the position of this insertion, hypoxia treatment (4 hr) of *nip2;1* plants resulted in poor expression of *NIP2;1* compared to wild type plants (Fig. 2B). Assay of NIP2;1 protein levels by Western blot showed no detectable NIP2;1 protein in root tissues of *nip2;1* mutant plants after 6 hours of hypoxia compared to wild type plants (Fig. 2C).

To determine the effects of low oxygen stress on *nip2;1* plants, their growth and survival under normoxic and hypoxic conditions were compared (Fig. 3). While wild type and *nip2;1* plants showed little difference in growth under normoxic conditions (Supplemental Fig 2), *nip2;1* plants showed higher sensitivity to hypoxia treatment (Fig. 3). After exposure to argon gas-induced hypoxia, followed by transfer back to normoxic conditions, *nip2;1* seedlings exhibited a higher incidence of leaf chlorosis within 24 hours after the hypoxia treatment (Fig. 3A). Comparison of the overall survival frequency of wild type and *nip2;1* seedlings showed that the mutant exhibited significantly poorer survival to hypoxic stress (Fig. 3C).

To confirm that the increased sensitivity of *nip2;1* plants to hypoxia is result of the loss of *NIP2;1* gene, complementation lines containing a *NIP2;1pro::NIP2;1-GFP* transgene in the *nip2;1* background were analyzed (Fig. 3C and Supplemental Fig. 2). The complementation

lines showed enhanced tolerance to hypoxia challenge compared to *nip2;1* plants, (Supplemental Figure 2), and were not statistically different to wild type plants with respect to survival frequency (Fig. 3C).

The sensitivity of the *nip2;1* mutant to hypoxia was further assessed by measuring the chlorophyll fluorescence properties and calculating the maximum potential quantum efficiency (Q_{max} or F_v/F_m) of photosystem (PS) II of *nip2;1* and WT seedlings under normal and low oxygen stress conditions. Chlorophyll fluorescence measurements is a common technique used to assess the photosynthetic efficiency of PS II which is an index of the susceptibility of plants to different environmental stressors (Murchie and Lawson, 2013). Under normoxic conditions, WT and *nip2;1* seedlings were not significantly different with F_v/F_m values that fell within the optimum range (0.78 - 0.8, Murchie and Lawson, 2013). This suggests that the lack of *NIP2;1* expression in the mutant line does not exhibit any detectable adverse effect on this parameter under standard growth conditions. However, upon hypoxia treatment both WT and *nip2;1* showed a steep reduction in photosynthetic efficiency with the F_v/F_m ratio declining to below 0.6 within four hours of the recovery period (Fig. 3B). At all time points, the F_v/F_m ratio is lower for *nip2;1* than wild type plants. At later time points the quantum efficiency of PS II starts to recover (Fig. 3C), but the *nip2;1* F_v/F_m ratio remains significantly lower than wild type after 24 hours of recovery.

Taken together, the *nip2;1* phenotype data indicate that *NIP2;1* is hypoxia core response protein that participates in the hypoxia adaptation response, and that reduction in expression of *NIP2;1* lowers the ability of Arabidopsis to survive this stress.

NIP2;1 is expressed on the plasma membrane as well as on internal membranes during hypoxia and reoxygenation recovery To investigate the dynamics of protein expression and the subcellular localization of NIP2;1, the *NIP2;1pro::NIP2;1-GFP* complementation lines were analyzed. Similar to wild type *NIP2;1*, Q-PCR analysis shows that the *NIP2;1-GFP* transgene transcript is acutely induced by hypoxia, with a peak at 4 hr followed by a decline (Fig. 4C). As

has been documented with other core hypoxia transcripts(Branco-Price et al., 2008), reoxygenation results in a rapid decline of the transcript to basal levels. Analysis of NIP2;1-GFP protein accumulation during hypoxia and re-oxygenation was done by using epifluorescence microscopy and Western blot analysis at different time points of hypoxia stress and reoxygenation recovery (Fig. 4A and B). The GFP signal first appeared within two hours of the onset of hypoxia (Fig. 4A and B), and increased as hypoxia proceeded. Return to normal oxygen conditions resulted in a substantial increase in the fluorescent intensity at 30 min (Fig. 4A) with Western blot protein levels peaking at 2 hr reoxygenation (Fig. 4B and C). While transcript levels decline rapidly to non-detectable levels (Fig. 4C), the fluorescent intensity and Western blot analyses indicate the persistence of the NIP2;1 protein for hours after return to normal oxygen conditions (Fig. 4A and B).

Different NIP proteins show varied subcellular localization, ranging from polarized plasma membrane localization for the root boric acid permease NIP5;1(Wang et al., 2017) to specific localization on subcellular organelles such as the soybean symbiosome membrane protein, nodulin 26 (Weaver et al., 1991). Previous work with NIP2;1 expression in heterologous systems with strong, constitutive non-native promoters suggested localization to either the plasma membrane (Choi and Roberts, 2007) or internal membranes (Mizutani et al., 2006). To investigate its subcellular localization under native conditions during hypoxia and reoxygenation, confocal microscopy of the roots of *NIP2;1pro::NIP2;1-GFP* seedlings was done (Fig. 5 and Supplemental Fig. 3).

Analysis of NIP2;1-GFP at 2 hr after the onset of hypoxia revealed accumulation within the elongation zone of the root with significant co-localization at the plasma membrane with the marker FM4-64 (Supplemental Fig. 3, Fig. 5), although some staining within internal structures is also apparent (Supplemental Fig. 3B). As hypoxia proceeds and more protein accumulates, the majority of NIP2;1-GFP signal appears to accumulate internally (Fig. 5, 6 hr time point).

Following 1 hr of reoxygenation, the localization of NIP2;1 on the surface appears to increase, although internal localization is still apparent (Fig. 5).

NIP2;1 participates in lactate efflux and media acidification during hypoxia Based on the specificity of NIP2;1 as a lactic acid permease based on biochemical analyses (Choi and Roberts, 2007), its localization in part to the surface of root cells, and the observation that hypoxia triggers release of lactate from roots into the external media (Xia and Saglio, 1992; Dolferus et al., 2008; Engqvist et al., 2015), it is hypothesized that NIP2;1 may participate in the excretion of lactate during the low oxygen stress response. To test this hypothesis, the pH and concentration of lactic acid within the media of wild-type and *nip2;1* seedlings challenged with hypoxia were examined. To compare the hypoxia-induced acidification of the external medium, 10 d-old wild-type and *nip2;1* seedlings were subjected to argon gas treatment on media containing the pH sensitive dye, bromocresol purple (Fig. 6A). Upon transfer from normoxic to hypoxic conditions, wild type plants show significant acidification of the media surrounding the roots, while *nip2;1* plants show no difference in bromocresol purple staining between normoxic and hypoxic conditions (Fig 6A).

In follow up analyses, the lactate levels released into the media by the roots of hypoxia-challenged wild type and *nip2;1* seedlings were compared. Wild type roots excrete significantly higher amounts of lactate into the environment compared with the roots of *nip2;1* plants (Fig 6B). The levels of lactate that accumulate within wild type and *nip2;1* roots tissues under hypoxic conditions were also compared (Fig. 6C). During a hypoxia time course, lactate levels increase in both wild type and *nip2;1* roots, but at all time points, including normoxia, *nip2;1* plants accumulate significantly higher levels of this metabolite (Fig. 6C). The results, combined with previous functional studies (Choi and Roberts, 2007), suggest that NIP2;1 is an endogenous lactic acid transporting channel protein that participates in lactate transport,

235 homeostasis, and efflux during low oxygen stress in Arabidopsis roots, and that this activity is
236 necessary to release lactate produced during anaerobic fermentation within the root.

237 **The loss of *NIP2;1* function affects the expression of pyruvate and lactate metabolic**
238 **enzymes** Anaerobic metabolism of pyruvate during oxygen limitation in plants occurs through
239 three conserved pathways: lactic acid fermentation, ethanolic fermentation and alanine
240 synthesis (Fig. 7). While all three pathways use pyruvate as a substrate, lactic acid and
241 ethanolic fermentation regenerate NAD^+, whereas alanine synthesis serves as a mechanism to
242 store nitrogen and carbon for reoxygenation (Sato et al., 2002; Ricoult et al., 2005). Genes that
243 encode enzymes in these pathways (such as *ADH*, *PDC, LDH*, and *AlaAT*) are among the "core
244 hypoxia response" proteins that are induced in Arabidopsis roots during hypoxia (Mustroph et
245 al., 2009; Lee et al., 2011; Mustroph et al., 2014). Conversely, L-lactate produced via LDH is
246 proposed to be converted back to pyruvate in peroxisomes (Fig. 7A) by the root-specific
247 glycolate oxidase 3 enzyme (Engqvist et al., 2015). Unlike other members of this enzyme family
248 that participate in the metabolism of glycolate, GOX3 is specific for L-lactate and utilizes oxygen
249 as an electron acceptor to oxidize lactate, producing hydrogen peroxide and pyruvate as end
250 products (Engqvist et al., 2015). *GOX3* is not a hypoxia-induced transcript and is rather
251 proposed to regulate the concentration of lactate in a coordinate fashion with LDH under aerobic
252 conditions (Engqvist et al., 2015; Maurino and Engqvist, 2015).

253 Q-PCR analysis shows that hypoxia response transcripts encoding fermentation
254 enzymes (*ADH1, PDC1, LDH,* and *AlaAT1*) show induction in root tissues during 4 hr of argon
255 gas (Fig. 7B). However, closer analysis of wild type and *nip2;1* roots show different levels of
256 selective transcripts. While *LDH* transcript levels show no statistical differences between wild
257 type and *nip2;1* roots, *ADH1, PDC1*, and *AlaAT1* are substantially elevated in *nip2;1* compared
258 to wild type plants (Fig. 7C). Conversely, *GOX3*, which is expressed at the same level under
259 normal and hypoxic conditions in wild type roots, is substantially reduced in hypoxic *nip2;1*
260 roots. Overall, the data suggest that the alterations in lactic acid homeostasis within the *nip2;1*

mutant have a selective effect on the metabolism of pyruvate and lactate metabolizing enzyme expression, with transcripts encoding fermentation enzymes in ethanol and alanine producing pathways enhanced, whereas the transcript that encodes the lactic acid metabolizing enzyme GOX3 is suppressed.

Discussion

NIP2;1-mediated lactic acid efflux promotes Arabidopsis survival during low oxygen stress In response to low oxygen conditions resulting from flooding or submergence stress, plants switch to anaerobic fermentation pathways to maintain glycolytic flux and energy production. In Arabidopsis, enzymes of ethanolic (ADH and PDC) and lactic acid (LDH) fermentation pathways are necessary for optimal survival to low oxygen stress(Ellis et al., 1999; Ismond et al., 2003; Kursteiner et al., 2003; Dolferus et al., 2008). The levels of lactate increase 14-fold within the root during the first two hours of hypoxia challenge (Mustroph et al., 2014) suggesting that lactic acid fermentation is induced during the initial stages of hypoxia. As lactate accumulates, hypoxia-stressed Arabidopsis plants (Dolferus et al., 2008), similar to other plant lineages (Xia and Saglio, 1992; Rivoal and Hanson, 1993; Xia and Roberts, 1994), efflux lactate from the roots to the external media/rhizosphere during low oxygen stress. Lactate efflux mechanisms in plant roots may assist in mitigating cellular acidification or other toxic effects of lactate accumulation during anaerobic stress (Xia and Roberts, 1994; Greenway and Gibbs, 2003).

To alleviate potential cellular acidification from lactate fermentation, the pathways for the efflux of lactic acid must transport either the protonated form (lactic acid) or co-transport lactate with a proton [reviewed in (Greenway and Gibbs, 2003)]. In the case of animal cells, lactate is effluxed or taken up by members of the SLC16 subgroup of the major facilitator superfamily known as Monocarboxylate Transporters or MCTs (Counillon et al., 2016; Sun et al., 2017). These proteins are symporters that co-transport lactate with H^+ in a bidirectional fashion. They

participate in the efflux of excess lactic acid during anaerobic fermentation, and also serve as an uptake mechanism for lactate from the serum for further metabolism (Sun et al., 2017). Land plants lack members of the SLC16/MCT transporter family, and the molecular identity of the transporters or channels that mediate the efflux of lactate/lactic acid produced during anaerobic fermentation have remained unclear. In this study, cellular, and genetic evidence is provided that, together with previous protein functional analyses (Choi and Roberts, 2007), indicate that the aquaporin-like NIP2;1 assists in mediating lactic acid efflux from Arabidopsis roots.

Nodulin Intrinsic Proteins are a plant-specific subgroup of the aquaporin superfamily that have diversified structurally and functionally during land plant evolution, and which have acquired solute transport activities beyond canonical aquaporin water transport (Roberts and Routray, 2017). NIP transport functions range from glycerol to ammonia to metalloid metabolites such as boric and silicic acid. However, biophysical and biochemical analysis of Arabidopsis NIP2;1 in Xenopus oocytes (Choi and Roberts, 2007) indicate that it is an outlier from other classical NIP proteins and is impermeable to water and all traditional NIP solute substrates, and instead shows specific bidirectional permeability to protonated lactic acid. Several observations in the present work provide strong support that lactic acid transport and efflux is the biological function of NIP2;1. First, the expression of NIP2;1 in response to hypoxia coincides with the appearance of lactate in the external medium; second, genetic mutation of the NIP2;1 via T-DNA insertion results in the reduction of lactate efflux from hypoxic roots into the external medium and a concomitant increase in the accumulation of lactate within root tissue; and third, mutant *nip2;1* plants show reduction in the acidification of the media surrounding hypoxic roots.

Mutant *nip2;1* plants show poorer survival to argon-induced low oxygen stress compared to wild type plants, presumably because of the over accumulation of toxic levels of lactic acid due to a reduced ability to efflux this end product from roots. As noted above, cytosolic lactate generation would increase the acid load of the cytosol that could contribute to acidosis (Davies

et al., 1974; Roberts et al., 1984; Felle, 2005). Additionally, the accumulation of lactate could also contribute to reduced glycolytic flux by affecting NAD^+ regeneration by altering the equilibrium of the LDH reaction, or potentially through product feedback inhibition mechanisms. For example, recent studies in yeast and mammals show that over accumulation of lactate leads to the production of the toxic side product 2-phospholactate catalyzed by pyruvate kinase. This side product of lactate blocks the production of fructose-2-6 bisphosphate, leading to the inhibition of the key glycolytic enzyme phosphofructokinase-1 (Collard et al., 2016). The production of similar toxic lactate metabolites side products could conceivably occur in plant tissues as well.

NIP2;1 expression during normoxia, hypoxia stress and recovery NIP2;1 expression is almost completely limited to root tissues with a precise pattern of transcript and protein expression during normoxic, hypoxic, and reoxygenation conditions. Under normoxic conditions, *NIP2;1* promoter activity is restricted to cells within the stele of the mature root (Supplemental Fig. 1). The cells of the stele are hypoxic even under well aerated growth conditions due to the low rate of lateral oxygen diffusion across the mature differentiated root (Armstrong et al., 1994; Gibbs and Greenway, 2003). “Anoxic cores" in the root stele are proposed to aid in hypoxia sensing and acclimation, potentially by the communication of low oxygen or energy signals (ethylene, metabolites, low pH, and Ca^{2+}) between hypoxic and well-aerated cells (Armstrong et al., 2019). The roots of *nip2;1* mutants show increased accumulation of lactate under normoxic conditions (Fig. 6C). This suggests that LDH is active in anoxic core tissues, even under aerobic conditions, and that NIP2;1 basal expression is necessary for maintaining low lactate accumulation.

NIP2;1 Q-PCR and GUS data show the characteristics of a core hypoxia response transcript, with acute induction of *NIP2;1* expression in roots within 1 hr of the initiation of hypoxia stress, followed by a peak and eventual decline to a reduced but elevated steady state level that is sustained during hypoxia. Interestingly, examination of the cell-specific translatome

338 atlas based on the work of (Mustroph et al., 2009) shows that the expression *NIP2;1* during
339 hypoxia parallels the expression of the two lactate metabolizing enzyme transcripts, *LDH* and
340 *GOX3* (Supplemental Figure 4). All three transcripts are predominantly, if not exclusively,
341 expressed in root tissue (Dolferus et al., 2008; Mustroph et al., 2014; Engqvist et al., 2015), and
342 accumulate to the highest levels in the root cortex, as well as to high levels within the epidermal
343 and vascular tissues, but are absent or poorly expression in leaf tissues. The root-predominant
344 expression pattern of *NIP2;1, LDH1* and *GOX3* is consistent with the distinct lactate metabolic
345 properties and responses of roots and shoots to low oxygen stress (Ellis et al., 1999; Mustroph
346 et al., 2014). Based on the model of (Engqvist et al., 2015), these three gene products are
347 proposed to coordinate lactate homeostasis through its production (LDH), its recovery back to
348 pyruvate (GOX3), and the excretion of lactate from the cell when it is overproduced during low
349 oxygen stress (NIP2;1).

350 Similar to other hypoxia-induced genes (Branco-Price et al., 2008), reoxygenation
351 results in suppression of *NIP2;1* mRNA expression and a return to low basal levels within two
352 hours of recovery. In contrast, NIP2;1 protein levels increase during early reoxygenation and
353 remain elevated for several hours post recovery, suggesting that the activity of the protein is
354 also required during recovery. In addition to excretion of lactic acid to the media, Arabidopsis
355 can take up L-lactate from the media and metabolize it (Dolferus et al., 2008; Engqvist et al.,
356 2015). Since NIP2;1 mediates the bidirectional flux of lactic acid (Choi and Roberts, 2007), it
357 could assist in the recovery of excreted lactic acid to trigger its metabolism to pyruvate and entry
358 into the TCA cycle as part of the replenishment of TCA cycle intermediates that takes place
359 during post-anoxic recovery(Branco-Price et al., 2008; Tsai et al., 2014; Yeung et al., 2019).

360 **NIP2;1 localization during hypoxia stress and recovery** By using the complementation lines
361 with a *NIP2;1-GFP* transgene under the native promoter, the localization of the protein during
362 hypoxia stress and recovery was analysed. NIP2;1-GFP shows a strong colocalization with a

plasma membrane marker during early hypoxia when the protein starts to appear (2 hrs). During extended hypoxia (>6 hr) the NIP2;1 GFP signal becomes stronger, and with enhanced localization within endomembranes although expression on the cell surface is still observed. During recovery, dual localization is still observed, although plasma membrane localization appears to be prevalent. These observations indicate that the NIP2;1 is distributed to both surface and internal membranes, and can explain the potential conflicting reports of different subcellular localization (plasma membrane and ER) based on transient expression in Arabidopsis protoplasts under the CaMV promoter in earlier work (Mizutani et al., 2006; Choi and Roberts, 2007). Subsequent analysis of NIP2;1-GFP localization in transgenic Arabidopsis plant roots driven by a heterologous NIP5;1 promoter under aerobic conditions, also showed dual localization (Wang et al., 2017).

The trafficking of plant aquaporins to various target membranes through endocytic and redistribution pathways is regulated based on metabolic need and stress physiology [reviewed by (Chevalier and Chaumont, 2015; Takano et al., 2017)]. For example, PIP2;1 aquaporins are dynamically cycled between the internal membranes and the plasma membrane (Li et al., 2011), with regulation via phosphorylation (Boursiac et al., 2008; Prak et al., 2008) or other factors (Santoni, 2017; Takano et al., 2017) leading to preferential surface expression or internalization, which regulates the hydraulic conductivity of the cell. The dual localization of NIP2;1 could reflect a similar dynamic distribution and trafficking between internal membranes and the cell surface to regulate lactate efflux. In the case of some plant (Prak et al., 2008) as well as mammalian (Noda and Sasaki, 2006) aquaporins, preferential trafficking to the plasma membrane is controlled by the phosphorylation of serine within the cytosolic carboxyl terminal domain. Proteins of the NIP I subgroup are phosphorylated on a homologous serine within the carboxyl terminal domain (Wallace et al., 2006; Santoni, 2017), which is catalyzed by CDPK/CPK kinases (Weaver et al., 1991). This phosphorylation motif is conserved in NIP2;1 (Ser 278). In addition, phosphoproteomic analysis reveals that NIP2;1 is also phosphorylated in

389 the N-terminal domain at Ser 5 by an unidentified protein kinase (Vialaret et al., 2014). Whether
390 phosphorylation, or other regulatory factors, control trafficking or distribution of NIP2;1 in
391 response to hypoxia or recovery signals to regulate lactic efflux or uptake remains to be
392 investigated.
393 **Lactic acid and ethanolic fermentation pathways** Ethanolic fermentation through the PDC-
394 catalyzed decarboxylation of pyruvate followed by subsequent production of ethanol from
395 acetaldehyde via ADH is proposed to be the major anaerobic catabolism pathway (Gibbs and
396 Greenway, 2003). However, lactic acid fermentation is also carried out in most plant species
397 (Gibbs and Greenway, 2003), and in many cases may precede, and regulate the transition to
398 ethanolic fermentation. The reason for initial reliance on lactic acid fermentation during hypoxia
399 prior to a shift to ethanolic fermentation is not clear (Gibbs and Greenway, 2003). However, this
400 pathway, unlike ethanolic fermentation, could allow recovery of the fermentation end product.
401 Additionally, lactate production via LDH occurs under aerobic conditions in response to other
402 abiotic and biotic stresses that could affect energy metabolism (Dolferus et al., 2008; Maurino
403 and Engqvist, 2015). In animal systems, the physiological role of lactate transcends serving as
404 an end product for anaerobic glucose metabolism, and its larger role as a metabolic regulator
405 has emerged, including G-protein signalling as well as transcriptional regulation through histone
406 modification (Latham et al., 2012; Sun et al., 2017; Zhang et al., 2019).
407 The possibility of lactate as a signal in plant systems remains largely unexplored.
408 Nevertheless, there is evidence that the balance between the two fermentation pathways is
409 regulated. For example, in classical studies of maize root tips, plants subjected to hypoxia
410 stress initially engage in lactic acid fermentation followed by a switch to primarily ethanolic
411 fermentation that is proposed to be driven by cellular acidification by lactate accumulation or
412 other means that results in subsequent pH-dependent activation of PDC [the “pH stat” model
413 (Davies et al., 1974; Roberts et al., 1984)]. In the case of Arabidopsis, overexpression of *LDH*
414 results in an increase in PDC activity and media efflux of lactate (Dolferus et al., 2008),

suggesting that increased lactic acid fermentation triggers the expression of ethanolic fermentation enzymes. Conversely, *adh1* null plants induce higher levels of lactic acid production to apparently compensate for reduced flux through the ethanolic fermentation pathway (Ismond et al., 2003). In *nip2;1* mutants, the accumulation of higher tissue lactate may produce an effect similar to *LDH1* overexpression. Higher transcript levels encoding enzymes within alternative pathways of the metabolism of pyruvate (e.g., *PDC1*, *ADH1* and *AlaAT1*) may be an adaptive response to the accumulation of lactic acid in *nip2;1* roots.

The reason for the selective reduction of *GOX3* inhibition in hypoxic *nip2;1* roots is less clear. As pointed out by Engqvist et al. (2015), the proposed role of this enzyme is to convert lactate back to pyruvate within the peroxisome which would serve to reduce lactic acid levels within the cell. Notably, however, this conversion occurs with the production of a reactive oxygen end product (hydrogen peroxide). ROS production is a major contributor to reoxygenation stress and is associated with poor tolerance to hypoxia and recovery (Yeung et al., 2019). If cytosolic lactate levels are elevated in *nip2;1* mutants, GOX3 (which uses oxygen as a co-substrate) could trigger greater ROS production upon reoxygenation.

Aquaporins as lactic acid channels in other plant and microbial systems In addition to Arabidopsis NIP2;1, select aquaporins with lactic acid permeability and efflux function have been described in other systems. For example, the Lactobacillales, which produce large quantities of lactic acid through fermentation, possess isoforms of the glycerol facilitator encoded by the *GlpF1* and *GlpF4* that facilitate lactic acid efflux (Bienert et al., 2013). The human trematode pathogen, *Schistosoma mansoni*, which performs lactic acid fermentation during the pathogenic part of its life cycle, possesses a lactic acid permeable plasma membrane aquaporin SmAQP that is proposed to release this end product (Faghiri et al., 2010). More pertinent to the present study, recent work (Mateluna et al., 2018) has identified other NIP I proteins, PruavNIP1;1 and PrucxmNIP1;1, that are induced during low oxygen stress in hypoxia-tolerant *Prunus* root stocks, and which are proposed to be lactic acid permeable

proteins based on yeast lactate auxotroph assays. These observations suggest that a subset of the NIP I family have evolved to functionally flux lactic acid. Since NIP2;1 retains the ar/R pore constriction properties of other lactic acid-impermeable NIP aquaglyceroporins, the structural alterations within the pore that confer the altered selectivity for lactic acid and the exclusion of other substrates include additional pore determinants besides the canonical selectivity filter that remain to be elucidated. Finally, whether NIP proteins are part of a larger network of transporters that coordinate directional lactate efflux and movement within root tissues, similar to NIP and BOR proteins in boric acid homeostasis (Takano et al., 2008), remains unknown.

Materials and Methods

Plant growth conditions and stress treatments *Arabidopsis thaliana* ecotype Columbia-0 was used in all experiments. Seeds were sterilized and stratified at 4 °C for 2 days, and were germinated as in (Choi and Roberts, 2007). Seedlings were grown vertically on in Murashige-Skoog (MS) media supplemented with 1% (w/v) sucrose and 0.8% (w/v) Phyto-agar (plantMedia) with a long day (LD) cycle of 16 hours of light (100 μmol m^{-2} s^{-1}) and 8 hours of dark (LD conditions). Hypoxia treatment was administered at the end of the light cycle by the argon-treatment protocol described by (Lokdarshi et al., 2016). For normoxic controls, seedlings were treated simultaneously under identical conditions except in the presence of air instead of argon gas. Phenotype analysis for hypoxia survival was conducted as described by Lokdarshi et al. (2016) with modifications. Briefly, seven days old seedlings were administered 8 hours of argon gas-induced hypoxia or air, and were returned to LD growth conditions. The survival frequency (seedling chlorosis) was scored three days after stress treatment.

Photosynthetic efficiency measurement The maximum quantum yield of photosystem II [$QY_{max}= F_v /F_m$] was measured with a FluorCam 800MF instrument (Photon Systems Instruments) by the general method of (Murchie and Lawson, 2013). Seven-day old seedlings were administered 8 hr hypoxia, and QY_{max} was measured at different recovery time points

upon return to LD conditions. For the first time point (time=0), seedlings were removed from hypoxia and were subjected to a saturating pulse of 1800 µEin $m^{-2}s^{-1}$ for 0.8 sec (F_m). Variable fluorescence (F_v) was calculated as the difference between F_o and F_m to calculate the maximum quantum yield [F_v/F_m]. For subsequent measurements, seedlings were dark adapted for 2 min (F_0) prior to application of the saturating pulse and conducting measurements.

T-DNA Insertion Mutant *nip2;1* and complementation line A sequence tagged T-DNA insertion line within the *NIP2;1* gene (WiscDsLox233237_22k) from the WiscDs-Lox T-DNA collection (Woody et al., 2007) was obtained from Arabidopsis Biological Resource Center at the Ohio State University. The mutant, herein named *nip2;1*, was selected on MS media supplemented with 15 µg/mL Basta. The genotype of mutant plants was assessed by a PCR-based genotyping protocol as described at (http://signal.salk.edu/tdnaprimers.2.html). For this purpose, genomic DNA was extracted from 2-wk old seedlings using the *Wizard* Genomic DNA purification kit (Promega) and was subjected to PCR analysis using two *AtNIP2;1* gene specific primers and the left border T-DNA primer (all primers used in this study are described in Supplemental Table 1). The precise site of T-DNA insertion was verified by a cloning of the PCR product into the pCR2.1-TOPO vector (Invitrogen) followed by automated DNA sequencing. All sequencing was performed at the University of Tennessee Molecular Biology Resource Facility. T4 homozygous mutant seedlings were used for all phenotyping and other analyses in this study.

For complementation of *nip2;1*, as well as to provide a mechanism for localization of a native protein construct by fluorescence microscopy, transgenic lines containing a transgene consisting of a *NIP2;1-GFP* translational fusion under the control of the *NIP2;1* promoter were generated in the *nip2;1* background. The promoter region of the *NIP2;1* gene (from the translational start site to a site 2000 bp upstream) was generated by PCR of Arabidopsis genomic DNA with gene specific primers with added *Kpn*I and *AatII* restriction sites

(Supplemental Table 1) to facilitate insertion into the binary vector pKGW_RedRoot_OCSA (Niyikiza et al., 2020). The modified destination vector was named pKGW_OCSA_*NIP2;1Pro*. The *NIP2;1* coding sequence (CDS) was amplified from the cDNA prepared from 4 hr hypoxic Arabidopsis seedlings with gene-specific primers with *Xba*I and *EcoR*I sites (Supplemental Table 1) to facilitate cloning into the Gateway entry vector CD3-1822 (Wang et al., 2013) to generate a construct of encoding NIP2;1 as an in-frame carboxyl-terminal fusion with GFP separated by a 3X Gly linker. The *NIP2;1-GFP* construct was then recombined into the pKGW_OCSA_*NIP2;1Pro* vector by using a gateway LR reaction (Invitrogen) to generate the final binary vector with $NIP2;1_{pro}$::*NIP2;1-GFP*. The constructs were sequenced and verified by using Snap Gene 4.2.11 software. *Agrobacterium tumefaciens* GV3101 (Koncz and Schell, 1986) was transformed with the final construct by electroporation with a Bio-Rad Gene Pulser Xcell Electroporation system. Colonies carrying the correct construct were verified by PCR, and were used to transform Arabidopsis *nip2;1* plants by using floral dip method (Clough and Bent, 1998).Transgenic lines were selected on MS media supplemented with 25 µg/ml kanamycin, and were confirmed by PCR-based genotyping with transgene specific primers (Supplemental Table 1). Twelve transgenic lines were generated and the three with the highest *NIP2;1* transgene abundance were selected for further analysis. T_2 generation complementation lines were used for the studies.

RNA Purification and Quantitative PCR Total RNA was isolated from plant tissues by grinding on liquid nitrogen and extracted by PureLink Plant RNA Reagent (Invitrogen). RNA isolation and DNase treatment was carried out by Direct-zol RNA MiniPrep Plus Kit using the manufacturer's protocol (Zymo Research). Q-PCR was performed on a Bio-Rad IQ5 real-time PCR detection system by using iTaq Universal SYBR Green One-Step RT-qPCR kit (Bio-Rad Laboratories) according to the manufacturer's instructions. All gene specific primers used in this study are summarized in Supplementary Table 1. Quantitative expression analysis was

517 calculated by the comparative threshold cycle (Ct) method (Pfaffl, 2001). Either *UBQ10* or
518 *ACTIN2* transcripts were used as the reference C_t for calculating ΔC_t for target gene expression,
519 and standardization to a calibrator transcript ($\Delta\Delta C_t$) was done as described in (Choi and
520 Roberts, 2007). The specific calibrators described in the figure legends.
521 **Histochemical and microscopy techniques** GUS staining and clearing of *Arabidopsis*
522 *thaliana* lines with the *NIP2;1*$_{pro}$*:GUS* reporter transgene was done by the protocol of (Choi and
523 Roberts 2007), and stained tissues were imaged with a LEICA MZ16FA microscope (Leica
524 Microsystems.). For analysis of *NIP2;1* promoter activity in root cross-sections, GUS-stained
525 roots were dehydrated in ethanol and embedded in Technovit 7100 resin by the manufacturer's
526 (Kulzer GmbH) protocol. Cross sections (2.5 µm thickness) were generated from the mature
527 differentiated region of the primary root with a Reichert OMV3 microtome equipped with a glass
528 knife, and were mounted in 50% (w/v) glycerol. Cross-sections were imaged with a Nikon
529 ECLIPSE E600 microscope equipped with Micropublisher 3.3 and QCapture 2.60 software
530 (QImaging corporation).
531 Epifluorescence imaging of NIP2;1-GFP plants were captured with an Axiovert 200M
532 microscope (Zeiss) equipped with filters for GFP fluorescence (Zeiss; filter set 38 HE) and a
533 digital camera (Hamamatsu Orca-ER) controlled by the Openlab software (Improvision).
534 Subcellular localization analysis under hypoxia and reoxygenation was done by confocal
535 microscopy. Hypoxia treatment was done with the argon protocol described above, and
536 seedlings were removed from the plate and were incubated in 4 uM FM4-64 under hypoxic
537 conditions (Invitrogen) in darkness for 10 min. For reoxygenation, seedlings were returned to
538 aerobic conditions under light for 1 hr before staining and visualization. Imaging was performed
539 with a Leica SP8 white laser confocal microscope system at the Advanced Microscopy and
540 Imaging Center at The University of Tennessee, Knoxville. The 488-nm excitation filter was
541 used, and the emission filter for detection was set to 495 to 550 for GFP and 580 to 650 nm for
542 FM4-64. Confocal micrographs were captured with the Leica LASX software and uncompressed

543 images were exported and analyzed in ImageJ version 1.53a (Schneider et al., 2012) to adjust
544 the brightness and contrast of images, and to generate merged images.
545 **Immunochemical Techniques** Anti-NIP2;1 antisera were produced against a synthetic peptide
546 (GenScript) corresponding to the C-terminal sequence of NIP2;1
547 (CHKMLPSIQNAEPEFSKTGSSHKRV) following the immunization protocol of (Guenther et al.,
548 2003) with the exception that Titermax-Gold was substituted for Freund's adjuvants. Antibodies
549 were affinity purified on peptide resins as described in (Guenther et al., 2003).
550 For analysis of NIP2;1 protein in wild type and *nip2;1* mutant after hypoxia treatment,
551 Arabidopsis root tissues from seedlings treated with 6 hr hypoxia or normoxic controls were
552 extracted, a membrane microsomal fraction was prepared as described by (Ishikawa et al.,
553 2005). Protein concentrations were determined by using the BCA assay (Pierce Biochemical).
554 The SDS-gel electrophoresis and Western blot analysis were performed using 10 µg protein
555 from membrane microsomal fractions as previously described (Guenther et al., 2003). For the
556 analysis of NIP2;1-GFP expression in complementation lines, hypoxia and reoxygenation
557 treatments were conducted as described above, and samples were directly extracted into SDS-
558 PAGE sample buffer (Laemmli, 1970) for Western blot analysis. Rabbit anti-GFP polyclonal
559 antibodies (Abcam) were used for the detection of NIP2;1-GFP.
560 **Media Acidification and L-Lactate Measurements** Media acidification assays with the pH-
561 sensitive indicator bromocresol purple was done by the method of (Silva et al., 2018). Seven
562 day wild type and *nip2;1* seedlings were transferred from MS media to 1.5% agarose plates
563 containing 60 mg L^{-1} Bromocresol Purple (Acros Organics) and 1mM $CaSO_4$ in sterile distilled
564 water with the pH adjusted to 5.7 using KOH . The bromocresol purple plates with the seedlings
565 were subjected to anaerobic condition as described above for 8 hrs before the images were
566 captured with a DSLR camera (Canon Rebel XS).

567 To quantify the L-lactate efflux from roots to the external media, seven-day old wild type
568 and *nip2;*1 7-d-old seedlings were transferred to Eppendorf tubes, with roots submerged in 1mL
569 of HPLC water, and were subjected to argon gas treatment as described above. At the selected
570 time points the plant material was removed and the L-lactate levels were quantified
571 enzymatically (LDH) as described by (Marbach and Weil, 1967). To determine L-lactate
572 concentration within Arabidopsis roots, hypoxia treatment of seedlings was carried out, roots
573 were dissected, and tissues were snap frozen in liquid nitrogen. The frozen tissue was ground
574 in a mortar with a pestle and was extracted in two volumes of 1N perchloric acid and was
575 neutralized with potassium carbonate on ice prior to assay by the LDH method of (Bergmeyer
576 and Bernt, 1974). NADH production was assayed by the change in absorbance at 340 nm, with
577 background corrected from duplicate samples treated identically except for no added LDH
578 enzyme.
579
580 **Gene Accession Information** Accession number of the genes used in this study are
581 AT2g34390 (*NIP2;1*), AT4g33070 (*PDC1*), AT4g18360 (*GOX3*), AT1g17290 (*AlaAT1*),
582 AT1g77120 (*ADH1*), AT3g18780 (*ACTIN 2*), AT4g05320 (*UBIQUITIN 10*), AT4g17260 (*LDH1*).
583
584 **Supplemental data**

585 **Supplemental Figure 1** Cellular localization of *AtNIP2;1* promoter activity in the roots under
586 normoxic growth conditions.

587 **Supplemental Figure 2** Complementation of *nip2;1* T-DNA mutant with a *NIP2;1pro::NIP2;1-*
588 *GFP* construct.

589 **Supplemental Figure 3** Subcellular localization of NIP2;1-GFP in the roots of hypoxia

590 challenged 7-d-old *NIP2;1-GFP* complementation lines.

591 **Supplemental Figure 4** Comparison of hypoxia-induced expression of *NIP2;1* and lactate

592 metabolizing enzyme transcripts *LDH* and *GOX3*

593 **Supplemental Table 1** Oligonucleotide primers

594
595
596 Acknowledgements:

597 We appreciate the assistance and valuable contributions of the following undergraduate

598 students of the BCMB Department at the University of Tennessee, Knoxville: Samantha McIntire

599 for helping in phenotyping experiment, and Shivam Ishanpara for helping us in growing and

600 genotyping transgenic plants and preparing media for the experiments; and especially Clayton

601 Nunn who participated in initial localization experiments. We are thankful to Tessa Burch-Smith

602 and John Dunlap for assisting us in microscopy in initial studies, and Andreas Nebenfuehr for

603 allowing us to use his laboratory's dissecting and epifluorescence microscopes.

604

605 **Figure Legends**

606 **Figure 1 *NIP2;1* expression in Arabidopsis seedlings in response to oxygen deficit**. A.

607 Quantitative real-time RT-PCR (Q-PCR) analysis of NIP2;1 transcripts in root (filled squares)

608 and shoot (open squares) tissues during a hypoxia time course of two week old Arabidopsis

609 seedlings. The ΔCt value of AtNIP2;1 obtained from 0 hr of shoot sample was used as the

610 calibrator for ΔΔCt calculations. The graph in the insert shows a rescaled plot of NIP2;1

611 expression in shoot tissue. Error bars indicate the SD of three biological replicates. B. GUS

612 staining analysis of two-week old NIP2;1pro::GUS Arabidopsis seedlings subjected to the

613 oxygen deprivation conditions as in panel A. Top panel are representative whole seedlings

while the bottom panel shows root cross-sections. Scale bars are 1.0 mm for the top panel and 20 µm in the bottom panel**.**

Figure 2 Characterization of *nip2;1* T-DNA insertional mutant seedlings. A. schematic diagram showing the T-DNA insertion in *nip2;1* mutant line. The boxes in the upstream portion of the gene indicate Anaerobic Response Elements. **B.** Q-PCR results for *NIP2;1* expression in the roots of 7d-old wild type and *nip2;1* during hypoxia treatment. The ∆Ct value of *NIP2;1* expression in normoxic wild type roots was used as a calibrator for relative expression. Error bars show the SD of 3 biological replicates. **C.** Root extracts (10 µg protein/lane) were analyzed by Western blot with site-directed NIP2;1 antibodies. **0 hr**, normoxic control; **6 hr**, 6 hr hypoxia-treated plants.

Figure 3 Effects of oxygen deprivation on the survival of *nip2;1-1* T-DNA insertional mutant seedlings. A. Seven-day-old, vertically grown seedlings corresponding to the wild-type (WT) and *nip2;1* T-DNA insertional mutant (*nip2;1*) were subjected to 8 hrs of argon gas treatment and were allowed to recover under normal oxygen conditions for 72 hours. Scale bar = 1 cm **B.** PSII maximal quantum yield, QYmax (Fv/Fm) was calculated from chlorophyll fluorescence analysis of 16hr light, 8hr dark grown 7-days-old WT and *nip2;1* mutant seedlings treated with 8 hr argon in dark (hypoxia) or air control (normoxia). Error bars represent std. error of mean of five biological replicates. Statistical significance was assessed by student t-test analysis to the wild type survival value. (* represents $p<0.05$) **C.** Histogram showing the survival of seven day old WT, *nip2;1,* and *NIP2;1-GFP* complementation seedlings to 8 hr argon treatment represented as a box and whisker plot of % seedling survival. Each data point represents one biological replicate with the median value indicated in each box. Statistical significance was assessed by student t-test analysis to the wild type survival value. (**** represents $p<0.0001$; ns, not significant).

Figure 4 NIP2;1-GFP expression in the roots of *NIP2;1:GFP* plants during hypoxia and reoxy- genation. Ten day old *NIP2;1-GFP* plants were subjected to an argon-induced hypoxia time course, with oxygen resupplied at hour 6. **A.** Representative epifluorescent images of the primary root of *NIP2;1:GFP* plants at the indicated times of hypoxia treatment or reoxygenation recovery. Scale bars = 50 µm. **B.** Anti-GFP Western blot showing NIP2;1-GFP protein accumulation (upper panel). The NIP2;1-GFP fusion protein and free GFP are indicated. Bottom panel, Coomassie blue stained loading control gel. **C.** Comparsion of root *NIP2;1-GFP* transcript levels (normalized to 0 hr) by Q-PCR (*left*) and NIP2;1-GFP protein based on densitometry of the Western blot in panel B.

Figure 5 Subcellular localization of NIP2;1-GFP in the roots of hypoxia challenged 7-d-old *NIP2;1-GFP* complementation lines. Seven-day-old vertically grown *NIP2;1-GFP* seedlings were subjected to anaerobic stress by root submergence under argon gas treatment followed by return to aerobic conditions at 6 hr. The appearance of NIP2;1 GFP was monitored at the times indicated by confocal fluorescence microscopy of the root elongation zone. FM4-64 staining was used to visualize the plasma membrane. DIC, differential interference contrast images. Bars = 50 µm.

Figure 6 Media acidification and lactic acid efflux in hypoxia-challenged *nip2;1* and wild type plants. A. Ten day-old *nip2;1* and wild-type (WT) seedlings were transferred to pH indicator plates containing bromocresol purple, and were subjected to 8 h treatment of hypoxia induced by argon gas **(Argon). Air** indicates a normoxic control. A color change from purple to yellow indicates a decrease in the pH of the environment. Scale bar = 1 cm. **B**. 10-d-old *nip2;1* and wild-type seedlings were submerged in water and subjected to argon gas treatment for 8 hr and the lactate concentration in the media was measured. Data are represented as a scatter plot of eight biological replicates with the horizontal line representing the mean and error bars showing the SE. **C.** Accumulation of lactate in seedlings based on enzymatic analysis during

hypoxia induced by bubbling nitrogen gas. Values are the average of three biological replicates at each timepoint, with the error bars showing the SEM. Asterisks indicate statistically significant differences based on a paired Student's t-test analysis (panel B) or One way ANOVA analysis (panel C).

Figure 7 Effect of *nip2;1* mutation on transcripts of pyruvate metabolism enzymes. A. Scheme showing the principal pathways of pyruvate and lactate metabolism during fermentation. **B.** Q-PCR analysis of the indicated transcripts in the roots of seven day old wild-type seedlings grown under normoxic conditions (black bars) or in response to 4 hr of argon-induced hypoxia (stripped bars). The data are normalized to the transcript levels of LDH under normoxic conditions (normalized expression = $2^{-\Delta\Delta Ct\text{-}LDH}$). Data are the average of nine replicates with the error bars showing the SD. **C.** Comparison of the hypoxia-induced changes of selected transcripts from the roots of wild type and *nip2;1* seedlings. The data were normalized to the expression levels of the indicated transcript under normoxic conditions. Data are the average of six determinations from three biological replicates with the error bars showing the SD. Asterisks indicate statistically significant differences based on an unpaired Student's t-test analysis.

References

Armstrong W, Beckett PM, Colmer TD, Setter TL, Greenway H (2019) Tolerance of roots to low oxygen: 'Anoxic' cores, the phytoglobin-nitric oxide cycle, and energy or oxygen sensing. Journal of Plant Physiology 239: 92-108

Armstrong W, Strange ME, Cringle S, Beckett PM (1994) Microelectrode and Modeling Study of Oxygen Distribution in Roots. Annals of Botany 74: 287-299

Bergmeyer HU, Bernt E (1974) Colorimetric Assay with l-Lactate, NAD Phenazine Methosulphate and INT. *In* HU Bergmeyer, ed, Methods of Enzymatic Analysis (Second Edition). Academic Press, pp 579-582

Bienert GP, Desguin B, Chaumont F, Hols P (2013) Channel-mediated lactic acid transport: a novel function for aquaglyceroporins in bacteria. Biochem J 454: 559-570

692 Boursiac Y, Prak S, Boudet J, Postaire O, Luu DT, Tournaire-Roux C, Santoni V, Maurel C
693 (2008) The response of Arabidopsis root water transport to a challenging environment
694 implicates reactive oxygen species- and phosphorylation-dependent internalization of
695 aquaporins. Plant Signal Behav 3: 1096-1098
696 Branco-Price C, Kaiser KA, Jang CJ, Larive CK, Bailey-Serres J (2008) Selective mRNA
697 translation coordinates energetic and metabolic adjustments to cellular oxygen
698 deprivation and reoxygenation in Arabidopsis thaliana. Plant J 56: 743-755
699 Branco-Price C, Kawaguchi R, Ferreira RB, Bailey-Serres J (2005) Genome-wide analysis of
700 transcript abundance and translation in Arabidopsis seedlings subjected to oxygen
701 deprivation. Ann Bot 96: 647-660
702 Chevalier AS, Chaumont F (2015) Trafficking of plant plasma membrane aquaporins: multiple
703 regulation levels and complex sorting signals. Plant Cell Physiol 56: 819-829
704 Choi WG, Roberts DM (2007) Arabidopsis NIP2;1, a major intrinsic protein transporter of lactic
705 acid induced by anoxic stress. J Biol Chem 282: 24209-24218
706 Clough SJ, Bent AF (1998) Floral dip: a simplified method for Agrobacterium-mediated
707 transformation of Arabidopsis thaliana. Plant J 16: 735-743
708 Collard F, Baldin F, Gerin I, Bolsee J, Noel G, Graff J, Veiga-da-Cunha M, Stroobant V,
709 Vertommen D, Houddane A, Rider MH, Linster CL, Van Schaftingen E, Bommer GT
710 (2016) A conserved phosphatase destroys toxic glycolytic side products in mammals
711 and yeast. Nat Chem Biol 12: 601-607
712 Counillon L, Bouret Y, Marchiq I, Pouyssegur J (2016) Na+/H+ antiporter (NHE1) and lactate/H+
713 symporters (MCTs) in pH homeostasis and cancer metabolism. Biochimica Et
714 Biophysica Acta-Molecular Cell Research 1863: 2465-2480
715 Davies DD, Grego S, Kenworthy P (1974) The control of the production of lactate and ethanol
716 by higher plants. Planta 118: 297-310
717 Dolferus R, Wolansky M, Carroll R, Miyashita Y, Ismond K, Good A (2008) Functional analysis
718 of lactate dehydrogenase during hypoxic stress in Arabidopsis. Functional Plant Biology
719 35: 131-140
720 Drew MC (1997) OXYGEN DEFICIENCY AND ROOT METABOLISM: Injury and Acclimation
721 Under Hypoxia and Anoxia. Annu Rev Plant Physiol Plant Mol Biol 48: 223-250
722 Ellis MH, Dennis ES, Peacock WJ (1999) Arabidopsis roots and shoots have different
723 mechanisms for hypoxic stress tolerance. Plant Physiol 119: 57-64
724 Engqvist MK, Schmitz J, Gertzmann A, Florian A, Jaspert N, Arif M, Balazadeh S, Mueller-
725 Roeber B, Fernie AR, Maurino VG (2015) GLYCOLATE OXIDASE3, a Glycolate

726 Oxidase Homolog of Yeast l-Lactate Cytochrome c Oxidoreductase, Supports l-Lactate
727 Oxidation in Roots of Arabidopsis. Plant Physiol 169: 1042-1061
728 Faghiri Z, Camargo SM, Huggel K, Forster IC, Ndegwa D, Verrey F, Skelly PJ (2010) The
729 tegument of the human parasitic worm Schistosoma mansoni as an excretory organ: the
730 surface aquaporin SmAQP is a lactate transporter. PLoS One 5: e10451
731 Felle HH (2005) pH regulation in anoxic plants. Annals of Botany 96: 519-532
732 Gibbs J, Greenway H (2003) Mechanisms of anoxia tolerance in plants. I. Growth, survival and
733 anaerobic catabolism (vol 30, pg 1, 1993). Functional Plant Biology 30: 353-U356
734 Giuntoli B, Lee SC, Licausi F, Kosmacz M, Oosumi T, van Dongen JT, Bailey-Serres J, Perata
735 P (2014) A trihelix DNA binding protein counterbalances hypoxia-responsive
736 transcriptional activation in Arabidopsis. PLoS Biol 12: e1001950
737 Greenway H, Gibbs J (2003) Mechanisms of anoxia tolerance in plants. II. Energy requirements
738 for maintenance and energy distribution to essential processes. Functional Plant Biology
739 30: 999-1036
740 Guenther JF, Chanmanivone N, Galetovic MP, Wallace IS, Cobb JA, Roberts DM (2003)
741 Phosphorylation of soybean nodulin 26 on serine 262 enhances water permeability and
742 is regulated developmentally and by osmotic signals. The Plant cell 15: 981-991
743 Ishikawa F, Suga S, Uemura T, Sato MH, Maeshima M (2005) Novel type aquaporin SIPs are
744 mainly localized to the ER membrane and show cell-specific expression in Arabidopsis
745 thaliana. FEBS Lett 579: 5814-5820
746 Ismond KP, Dolferus R, De Pauw M, Dennis ES, Good AG (2003) Enhanced low oxygen
747 survival in Arabidopsis through increased metabolic flux in the fermentative pathway.
748 Plant Physiology 132: 1292-1302
749 Johanson U, Karlsson M, Johansson I, Gustavsson S, Sjovall S, Fraysse L, Weig AR, Kjellbom
750 P (2001) The complete set of genes encoding major intrinsic proteins in Arabidopsis
751 provides a framework for a new nomenclature for major intrinsic proteins in plants. Plant
752 Physiol 126: 1358-1369
753 Kamiya T, Fujiwara T (2009) Arabidopsis NIP1;1 transports antimonite and determines
754 antimonite sensitivity. Plant Cell Physiol 50: 1977-1981
755 Kamiya T, Tanaka M, Mitani N, Ma JF, Maeshima M, Fujiwara T (2009) NIP1;1, an aquaporin
756 homolog, determines the arsenite sensitivity of Arabidopsis thaliana. J Biol Chem 284:
757 2114-2120

758 Koncz C, Schell J (1986) The promoter of TL-DNA gene 5 controls the tissue-specific
759 expression of chimaeric genes carried by a novel type of Agrobacterium binary vector.
760 Molecular and General Genetics MGG 204: 383-396
761 Kursteiner O, Dupuis I, Kuhlemeier C (2003) The pyruvate decarboxylase1 gene of Arabidopsis
762 is required during anoxia but not other environmental stresses. Plant Physiol 132: 968-
763 978
764 Laemmli UK (1970) Cleavage of structural proteins during the assembly of the head of
765 bacteriophage T4. Nature 227: 680-685
766 Latham T, Mackay L, Sproul D, Karim M, Culley J, Harrison DJ, Hayward L, Langridge-Smith P,
767 Gilbert N, Ramsahoye BH (2012) Lactate, a product of glycolytic metabolism, inhibits
768 histone deacetylase activity and promotes changes in gene expression. Nucleic Acids
769 Research 40: 4794-4803
770 Lee SC, Mustroph A, Sasidharan R, Vashisht D, Pedersen O, Oosumi T, Voesenek LA, Bailey-
771 Serres J (2011) Molecular characterization of the submergence response of the
772 Arabidopsis thaliana ecotype Columbia. The New phytologist 190: 457-471
773 Li X, Wang X, Yang Y, Li R, He Q, Fang X, Luu DT, Maurel C, Lin J (2011) Single-molecule
774 analysis of PIP2;1 dynamics and partitioning reveals multiple modes of Arabidopsis
775 plasma membrane aquaporin regulation. Plant Cell 23: 3780-3797
776 Licausi F, van Dongen JT, Giuntoli B, Novi G, Santaniello A, Geigenberger P, Perata P (2010)
777 HRE1 and HRE2, two hypoxia-inducible ethylene response factors, affect anaerobic
778 responses in Arabidopsis thaliana. Plant J 62: 302-315
779 Liu F, Vantoai T, Moy LP, Bock G, Linford LD, Quackenbush J (2005) Global transcription
780 profiling reveals comprehensive insights into hypoxic response in Arabidopsis. Plant
781 Physiol 137: 1115-1129
782 Lokdarshi A, Conner WC, McClintock C, Li T, Roberts DM (2016) Arabidopsis CML38, a
783 Calcium Sensor That Localizes to Ribonucleoprotein Complexes under Hypoxia Stress.
784 Plant Physiol 170: 1046-1059
785 Marbach EP, Weil MH (1967) Rapid enzymatic measurement of blood lactate and pyruvate. Use
786 and significance of metaphosphoric acid as a common precipitant. Clin Chem 13: 314-
787 325
788 Mateluna P, Salvatierra A, Solis S, Nunez G, Pimentel P (2018) Involvement of aquaporin
789 NIP1;1 in the contrasting tolerance response to root hypoxia in Prunus rootstocks. J
790 Plant Physiol 228: 19-28

Maurino VG, Engqvist MK (2015) 2-Hydroxy Acids in Plant Metabolism. Arabidopsis Book 13: e0182

Mizutani M, Watanabe S, Nakagawa T, Maeshima M (2006) Aquaporin NIP2;1 is mainly localized to the ER membrane and shows root-specific accumulation in Arabidopsis thaliana. Plant and Cell Physiology 47: 1420-1426

Murchie EH, Lawson T (2013) Chlorophyll fluorescence analysis: a guide to good practice and understanding some new applications. J Exp Bot 64: 3983-3998

Mustroph A, Barding GA, Jr., Kaiser KA, Larive CK, Bailey-Serres J (2014) Characterization of distinct root and shoot responses to low-oxygen stress in Arabidopsis with a focus on primary C- and N-metabolism. Plant Cell Environ 37: 2366-2380

Mustroph A, Lee SC, Oosumi T, Zanetti ME, Yang HJ, Ma K, Yaghoubi-Masihi A, Fukao T, Bailey-Serres J (2010) Cross-Kingdom Comparison of Transcriptomic Adjustments to Low-Oxygen Stress Highlights Conserved and Plant-Specific Responses. Plant Physiology 152: 1484-1500

Mustroph A, Zanetti ME, Jang CJ, Holtan HE, Repetti PP, Galbraith DW, Girke T, Bailey-Serres J (2009) Profiling translatomes of discrete cell populations resolves altered cellular priorities during hypoxia in Arabidopsis. Proc Natl Acad Sci U S A 106: 18843-18848

Niyikiza D, Piya S, Routray P, Miao L, Kim WS, Burch-Smith T, Gill T, Sams C, Arelli PR, Pantalone V, Krishnan HB, Hewezi T (2020) Interactions of gene expression, alternative splicing, and DNA methylation in determining nodule identity. Plant J

Noda Y, Sasaki S (2006) Regulation of aquaporin-2 trafficking and its binding protein complex. Biochim Biophys Acta 1758: 1117-1125

Pfaffl MW (2001) A new mathematical model for relative quantification in real-time RT-PCR. Nucleic Acids Res 29: e45

Pommerrenig B, Diehn TA, Bernhardt N, Bienert MD, Mitani-Ueno N, Fuge J, Bieber A, Spitzer C, Brautigam A, Ma JF, Chaumont F, Bienert GP (2020) Functional evolution of nodulin 26-like intrinsic proteins: from bacterial arsenic detoxification to plant nutrient transport. New Phytol 225: 1383-1396

Prak S, Hem S, Boudet J, Viennois G, Sommerer N, Rossignol M, Maurel C, Santoni V (2008) Multiple phosphorylations in the C-terminal tail of plant plasma membrane aquaporins: role in subcellular trafficking of AtPIP2;1 in response to salt stress. Mol Cell Proteomics 7: 1019-1030

823 Ricoult C, Cliquet J-B, Limami AM (2005) Stimulation of alanine amino transferase (AlaAT) gene
824 expression and alanine accumulation in embryo axis of the model legume Medicago
825 truncatula contribute to anoxia stress tolerance. Physiologia Plantarum 123: 30-39
826 Rivoal J, Hanson AD (1993) Evidence for a Large and Sustained Glycolytic Flux to Lactate in
827 Anoxic Roots of Some Members of the Halophytic Genus Limonium. Plant Physiol 101:
828 553-560
829 Roberts DM, Routray P (2017) The Nodulin26 Intrinsic Protein Subfamily. *In* F Chaumont, SD
830 Tyerman, eds, Plant Aquaporins From Transport to Signaling. Springer International
831 Publishing, pp 267-296
832 Roberts JK, Callis J, Jardetzky O, Walbot V, Freeling M (1984) Cytoplasmic acidosis as a
833 determinant of flooding intolerance in plants. Proc Natl Acad Sci U S A 81: 6029-6033
834 Santoni V (2017) Plant Aquaporin Postranslational Regulation. *In* F Chaumont, SD Tyerman,
835 eds, Plant Aquaporins From Transport to Signaling. Springer International Publishing, pp
836 83-105
837 Sato T, Harada T, Ishizawa K (2002) Stimulation of glycolysis in anaerobic elongation of
838 pondweed (Potamogeton distinctus) turions. J Exp Bot 53: 1847-1856
839 Schneider CA, Rasband WS, Eliceiri KW (2012) NIH Image to ImageJ: 25 years of image
840 analysis. Nat Methods 9: 671-675
841 Silva AL, Dressano K, Ceciliato PHO, Guerrero-Abad JC, Moura DS (2018) Evaluation of Root
842 pH Change Through Gel Containing pH-sensitive Indicator Bromocresol Purple. Bio-
843 Protocol 8(7):e2796
844 Sorenson R, Bailey-Serres J (2014) Selective mRNA sequestration by OLIGOURIDYLATE-
845 BINDING PROTEIN 1 contributes to translational control during hypoxia in Arabidopsis.
846 Proc Natl Acad Sci U S A 111: 2373-2378
847 Sun SR, Li H, Chen JH, Qian Q (2017) Lactic Acid: No Longer an Inert and End-Product of
848 Glycolysis. Physiology 32: 453-463
849 Takano J, Miwa K, Fujiwara T (2008) Boron transport mechanisms: collaboration of channels
850 and transporters. Trends Plant Sci 13: 451-457
851 Takano J, Yoshinari A, Luu D-T (2017) Plant Aquaporin Trafficking. *In* F Chaumont, SD
852 Tyerman, eds, Plant Aquaporins From Transport to Signaling. Springer International
853 Publishing, pp 47-81
854 Tsai KJ, Chou SJ, Shih MC (2014) Ethylene plays an essential role in the recovery of
855 Arabidopsis during post-anaerobiosis reoxygenation. Plant Cell Environ 37: 2391-2405

856 Vialaret J, Di Pietro M, Hem S, Maurel C, Rossignol M, Santoni V (2014) Phosphorylation
857 dynamics of membrane proteins from Arabidopsis roots submitted to salt stress.
858 Proteomics 14: 1058-1070
859 Voesenek LA, Bailey-Serres J (2013) Flooding tolerance: O2 sensing and survival strategies.
860 Curr Opin Plant Biol 16: 647-653
861 Voesenek LA, Bailey-Serres J (2015) Flood adaptive traits and processes: an overview. New
862 Phytol 206: 57-73
863 Wallace IS, Choi WG, Roberts DM (2006) The structure, function and regulation of the nodulin
864 26-like intrinsic protein family of plant aquaglyceroporins. Biochim Biophys Acta 1758:
865 1165-1175
866 Wang S, Yoshinari A, Shimada T, Hara-Nishimura I, Mitani-Ueno N, Feng Ma J, Naito S,
867 Takano J (2017) Polar Localization of the NIP5;1 Boric Acid Channel Is Maintained by
868 Endocytosis and Facilitates Boron Transport in Arabidopsis Roots. Plant Cell 29: 824-
869 842
870 Wang X, Fan C, Zhang X, Zhu J, Fu YF (2013) BioVector, a flexible system for gene specific-
871 expression in plants. BMC Plant Biol 13: 198
872 Weaver CD, Crombie B, Stacey G, Roberts DM (1991) Calcium-dependent phosphorylation of
873 symbiosome membrane proteins from nitrogen-fixing soybean nodules : evidence for
874 phosphorylation of nodulin-26. Plant Physiol 95: 222-227
875 Woody ST, Austin-Phillips S, Amasino RM, Krysan PJ (2007) The WiscDsLox T-DNA collection:
876 an arabidopsis community resource generated by using an improved high-throughput T-
877 DNA sequencing pipeline. J Plant Res 120: 157-165
878 Xia JH, Roberts J (1994) Improved Cytoplasmic pH Regulation, Increased Lactate Efflux, and
879 Reduced Cytoplasmic Lactate Levels Are Biochemical Traits Expressed in Root Tips of
880 Whole Maize Seedlings Acclimated to a Low-Oxygen Environment. Plant Physiol 105:
881 651-657
882 Xia JH, Saglio PH (1992) Lactic Acid efflux as a mechanism of hypoxic acclimation of maize
883 root tips to anoxia. Plant Physiol 100: 40-46
884 Xu W, Dai W, Yan H, Li S, Shen H, Chen Y, Xu H, Sun Y, He Z, Ma M (2015) Arabidopsis
885 NIP3;1 Plays an Important Role in Arsenic Uptake and Root-to-Shoot Translocation
886 under Arsenite Stress Conditions. Mol Plant 8: 722-733
887 Yeung E, Bailey-Serres J, Sasidharan R (2019) After The Deluge: Plant Revival Post-Flooding.
888 Trends Plant Sci 24: 443-454

889 Zhang D, Tang Z, Huang H, Zhou G, Cui C, Weng Y, Liu W, Kim S, Lee S, Perez-Neut M, Ding J,
890 Czyz D, Hu R, Ye Z, He M, Zheng YG, Shuman HA, Dai L, Ren B, Roeder RG, Becker L,
891 Zhao Y (2019) Metabolic regulation of gene expression by histone lactylation. Nature 574:
892 575-580
893

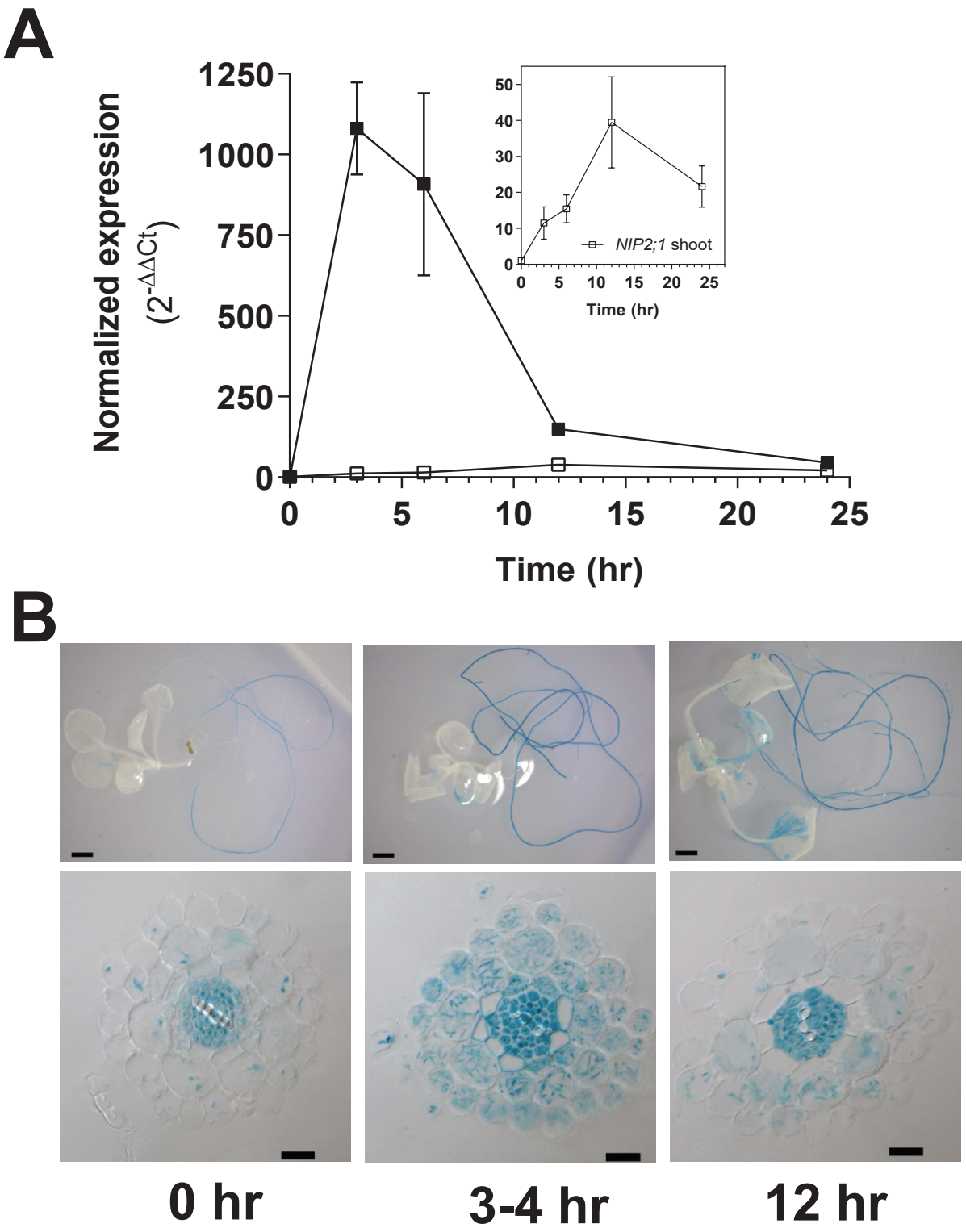

Figure 1 *NIP2;1* expression in Arabidopsis seedlings in response to oxygen deficit. A. Quantitative real-time RT-PCR (Q-PCR) analysis of *NIP2;1* transcripts in root (filled squares) and shoot (open squares) tissues during a hypoxia time course of two week old Arabidopsis seedlings. The ΔCt value of AtNIP2;1 obtained from 0 hr of shoot sample was used as the calibrator for ΔΔCt calculations. The graph in the insert shows a rescaled plot of *NIP2;1* expression in shoot tissue. Error bars indicate the SD of three biological replicates. **B.** GUS staining analysis of two-week old *NIP2;1*$_{pro}$*::GUS* Arabidopsis seedlings subjected to the oxygen deprivation conditions as in panel A. Top panel are representative whole seedlings while the bottom panel shows root cross-sections. Scale bars are 1.0 mm for the top panel and 20 μm in the bottom panel.

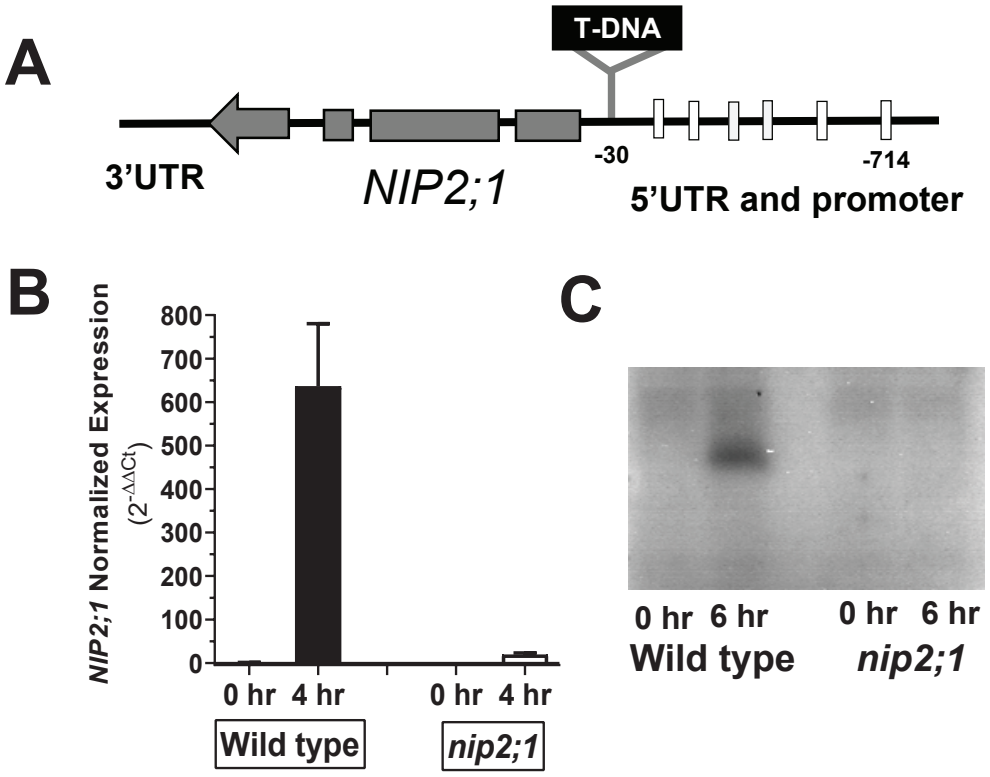

Figure 2 Characterization of *nip2;1* T-DNA insertional mutant seedlings. A. schematic diagram showing the T-DNA insertion in *nip2;1* mutant line. The boxes in the upstream portion of the gene indicate Anaerobic Response Elements. **B.** Q-PCR results for *NIP2;1* expression in the roots of 7d-old wild type and *nip2;1* during hypoxia treatment. The ΔCt value of *NIP2;1* expression in normoxic wild type roots was used as a calibrator for relative expression. Error bars show the SD of 3 biological replicates. **C.** Root extracts (10 µg protein/lane) were analyzed by Western blot with site-directed NIP2;1 antibodies. **0 hr**, normoxic control; **6 hr**, 6 hr hypoxia-treated plants.

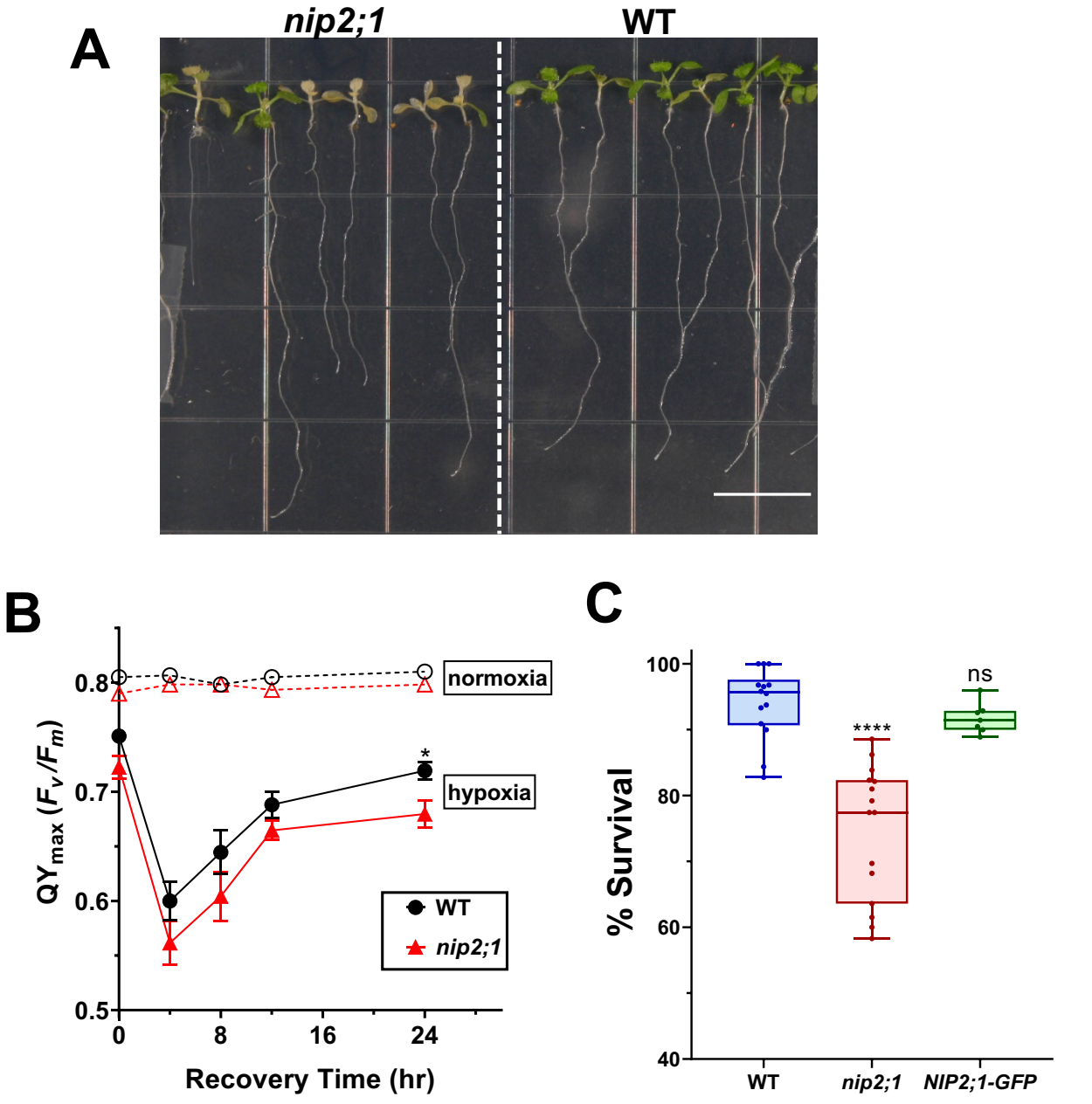

Figure 3 Effects of oxygen deprivation on the survival of *nip2;1-1* T-DNA insertional mutant seedlings. A. Seven-day-old, vertically grown seedlings corresponding to the wild-type (WT) and *nip2;1* T-DNA insertional mutant (*nip2;1*) were subjected to 8 hrs of argon gas treatment and were allowed to recover under normal oxygen conditions for 72 hours. Scale bar = 1 cm **B.** PSII maximal quantum yield, QY_{max} (F_v/F_m) was calculated from chlorophyll fluorescence analysis of 16hr light, 8hr dark grown 7-days-old WT and *nip2;1* mutant seedlings treated with 8 hr argon in dark (hypoxia) or air control (normoxia). Error bars represent std. error of mean of five biological replicates. Statistical significance was assessed by student t-test analysis to the wild type survival value. (* represents $p<0.05$) **C.** Histogram showing the survival of seven day old WT, *nip2;1,* and *NIP2;1-GFP* complementation seedlings to 8 hr argon treatment represented as a box and whisker plot of % seedling survival. Each data point represents one biological replicate with the median value indicated in each box. Statistical significance was assessed by student t-test analysis to the wild type survival value. (**** represents $p<0.0001$; ns, not significant).

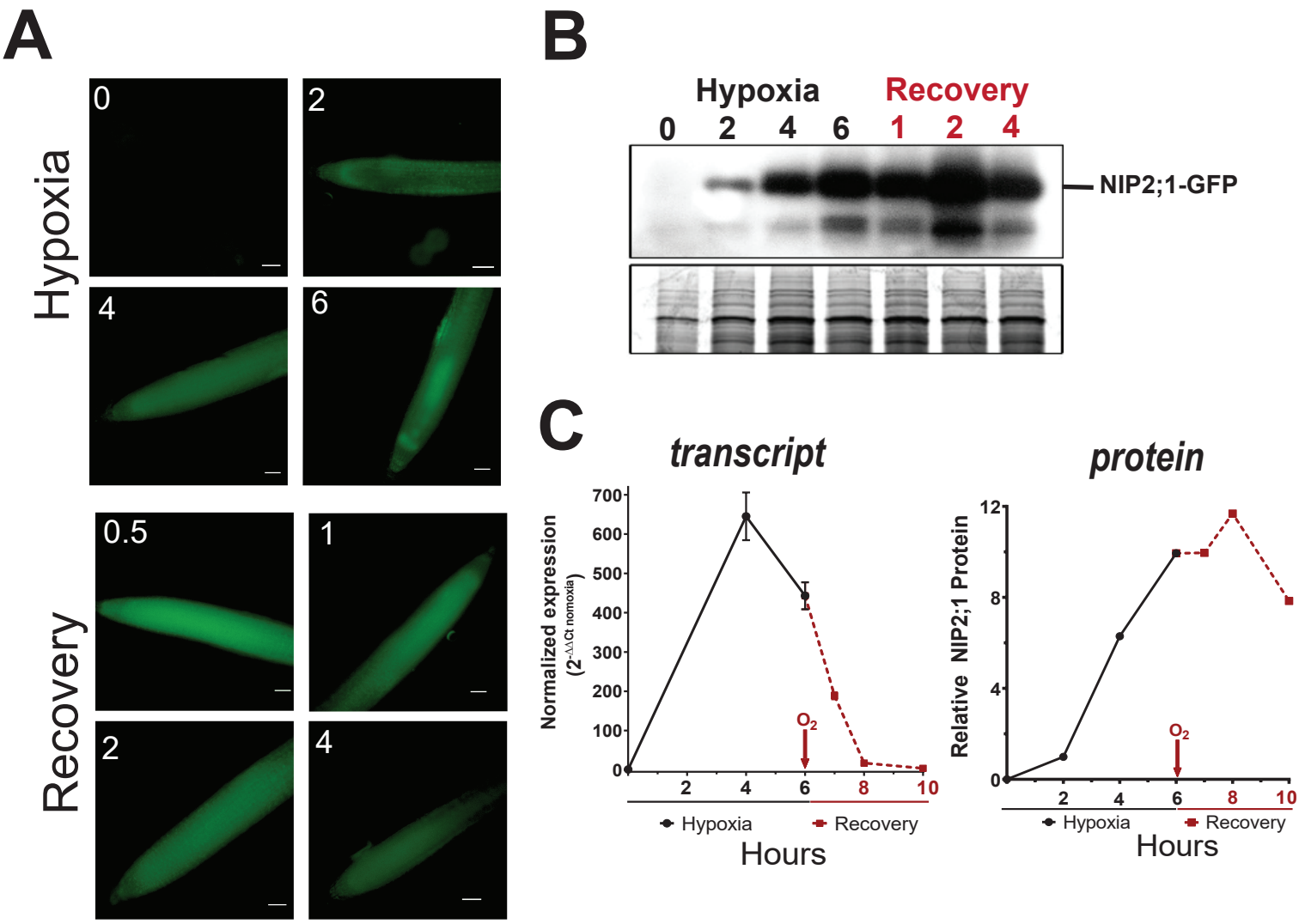

Figure 4 NIP2;1-GFP expression in the roots of *NIP2;1:GFP* plants during hypoxia and reoxygenation. Ten day old *NIP2;1-GFP* plants were subjected to an argon-induced hypoxia time course, with oxygen resupplied at hour 6. **A.** Representative epifluorescent images of the primary root of *NIP2;1:GFP* plants at the indicated times of hypoxia treatment or reoxygenation recovery. Scale bars = 50 µm. **B.** Anti-GFP Western blot showing NIP2;1-GFP protein accumulation (upper panel). Bottom panel, Coomassie blue stained loading control gel. **C.** Comparsion of root *NIP2;1-GFP* transcript levels (normalized to 0 hr) by Q-PCR (*left*) and NIP2;1-GFP protein based on densitometry of the Western blot iin panel B.

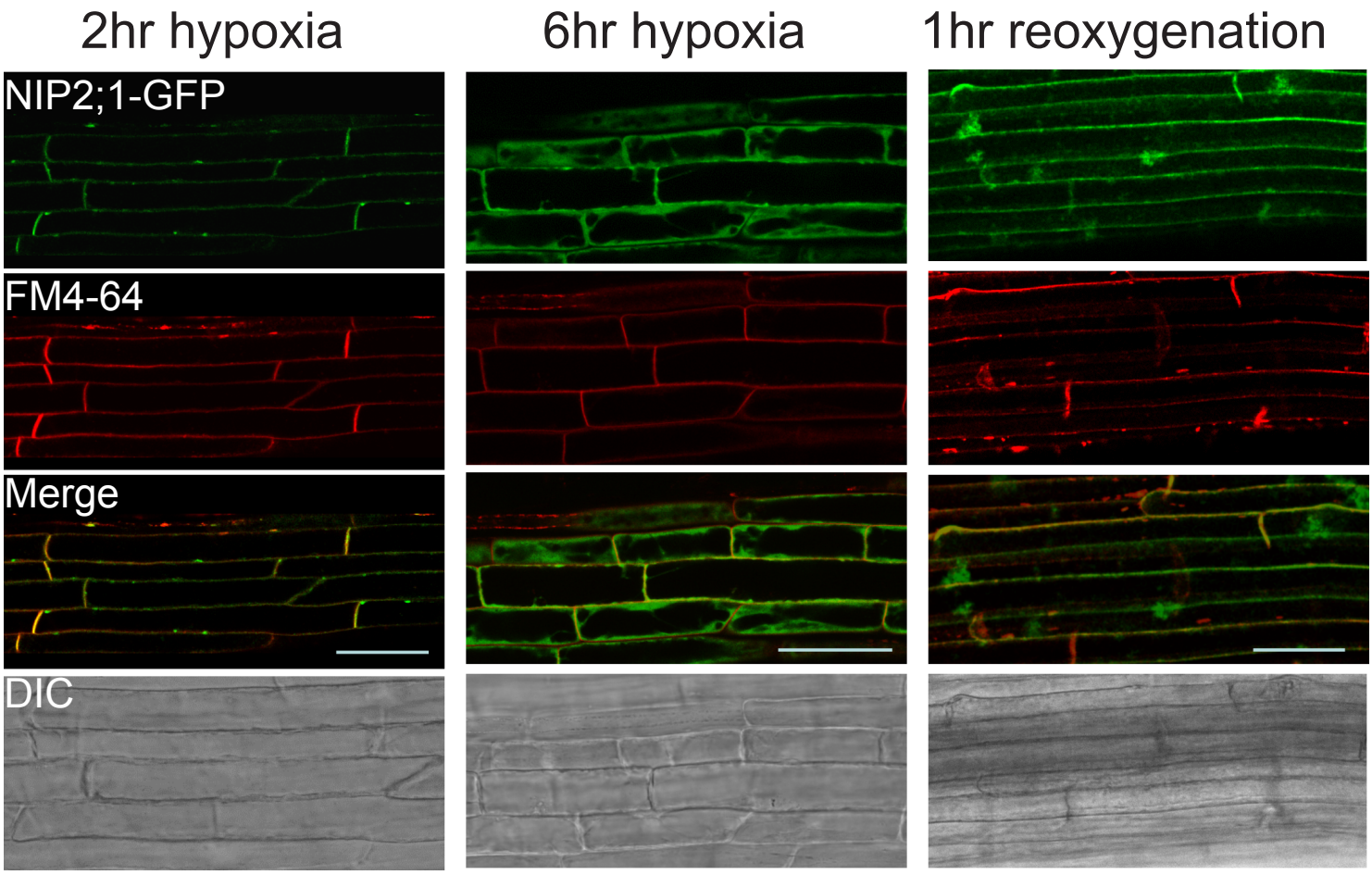

Figure 5 Subcellular localization of NIP2;1-GFP in the roots of hypoxia challenged 7-d-old *NIP2;1-GFP* complementation lines. Seven-day-old vertically grown *NIP2;1-GFP* seedlings were subjected to anaerobic stress by root submergence under argon gas treatment followed by return to aerobic conditions at 6 hr. The appearance of NIP2;1 GFP was monitored at the times indicated by confocal fluorescence microscopy of the root elongation zone. FM4-64 staining was used to visualize the plasma membrane. DIC, differential interference contrast images. Bars = 50 μm.

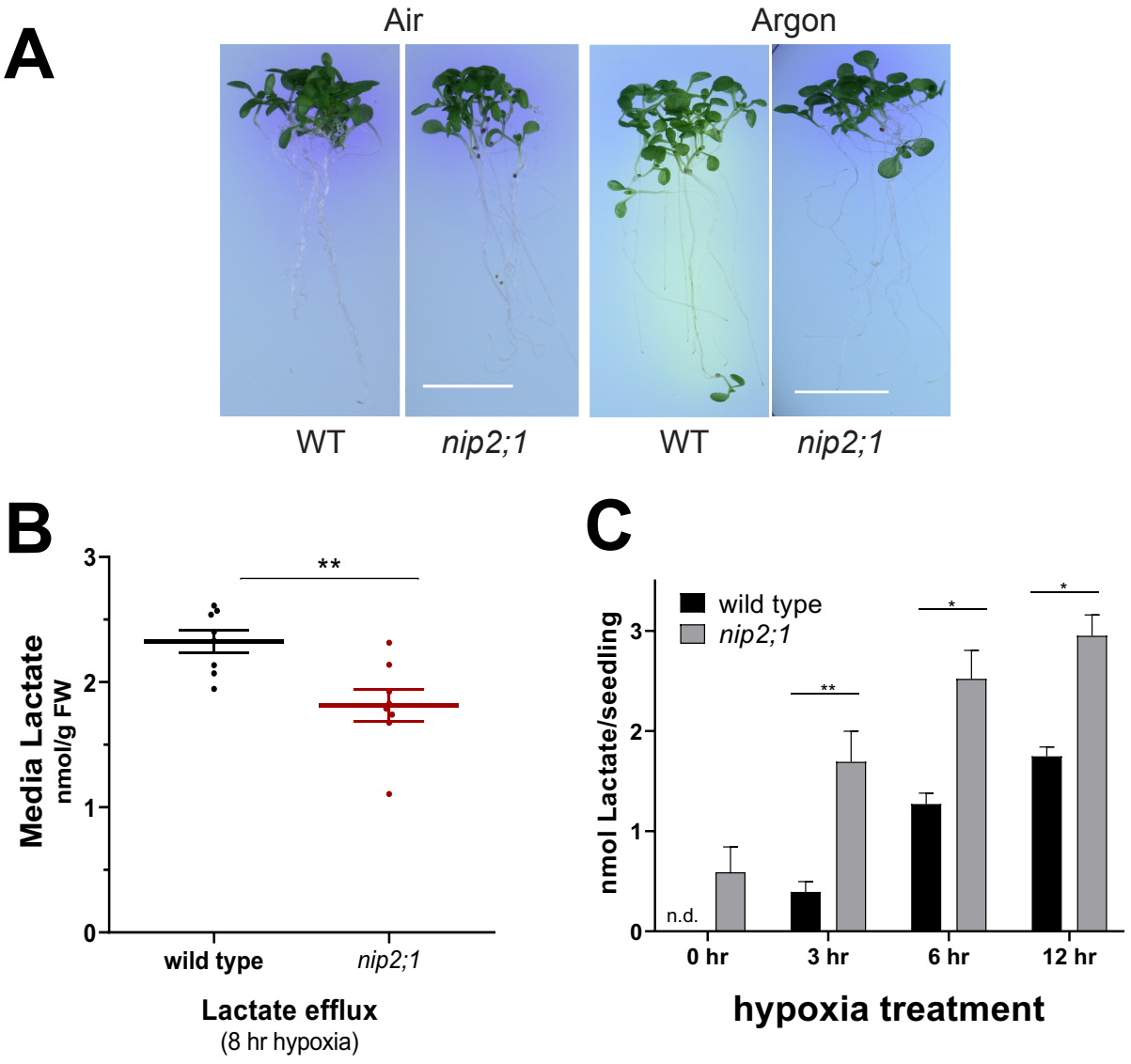

Figure 6 Media acidification and lactic acid efflux in hypoxia-challenged *nip2;1* and wild type plants. A. Ten day-old *nip2;1* and wild-type (WT) seedlings were transferred to pH indicator plates containing bromocresol purple, and were subjected to 8 h treatment of hypoxia induced by argon gas **(Argon). Air** indicates a normoxic control. A color change from purple to yellow indicates a decrease in the pH of the environment. Scale bar = 1 cm. **B**. 10-d-old *nip2;1* and wild-type seedlings were submerged in water and subjected to argon gas treatment for 8 hr and the lactate concentration in the media was measured. Data are represented as a scatter plot of eight biological replicates with the horizontal line representing the mean and error bars showing the SE. **C.** Accumulation of lactate in seedlings based on enzymatic analysis during hypoxia induced by bubbling nitrogen gas. Values are the average of three biological replicates at each timepoint, with the error bars showing the SEM. Asterisks indicate statistically significant differences based on a paired Student's t-test analysis (panel B) or One way ANOVA analysis (panel C).

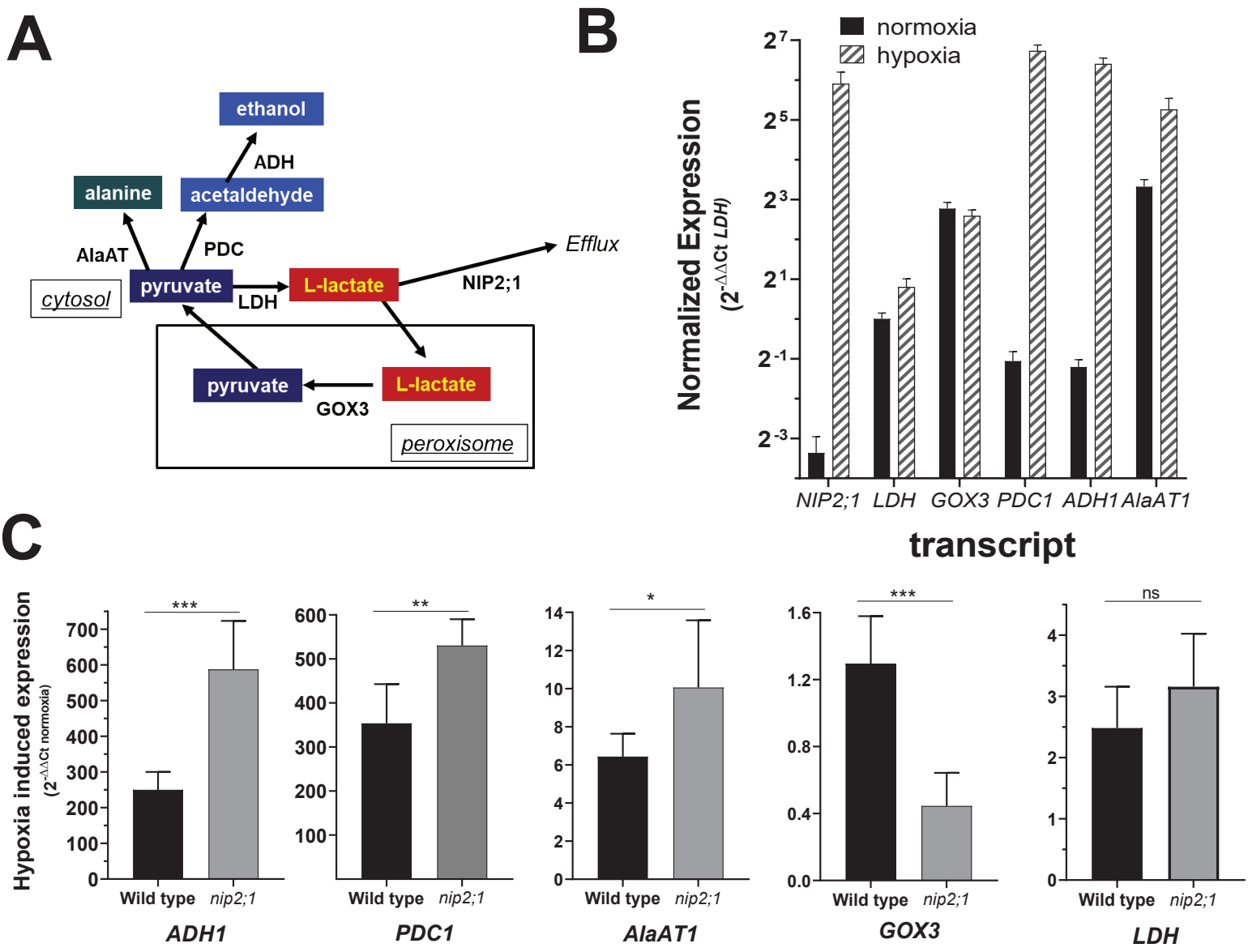

Figure 7 Effect of *nip2;1* mutation on transcripts of pyruvate metabolism enzymes. **A.** Scheme showing the principal pathways of pyruvate and lactate metabolism during fermentation. **B.** Q-PCR analysis of the indicated transcripts in the roots of seven day old wild-type seedlings grown under normoxic conditions (black bars) or in response to 4 hr of argon-induced hypoxia (stripped bars). The data are normalized to the transcript levels of LDH under normoxic conditions (normalized expression = $2^{-\Delta\Delta Ct\text{-}LDH}$). Data are the average of nine replicates with the error bars showing the SD. **C.** Comparison of the hypoxia-induced changes of selected transcripts from the roots of wild type and *nip2;1* seedlings. The data were normalized to the expression levels of the indicated transcript under normoxic conditions. Data are the average of six determinations from three biological replicates with the error bars showing the SD. Asterisks indicate statistically significant differences based on an unpaired Student's t-test analysis.

Parsed Citations

Armstrong W, Beckett PM, Colmer TD, Setter TL, Greenway H (2019) Tolerance of roots to low oxygen: 'Anoxic' cores, the phytoglobin-nitric oxide cycle, and energy or oxygen sensing. Journal of Plant Physiology 239: 92-108

Pubmed: Author and Title
Google Scholar: Author Only Title Only Author and Title

Armstrong W, Strange ME, Cringle S, Beckett PM (1994) Microelectrode and Modeling Study of Oxygen Distribution in Roots. Annals of Botany 74: 287-299

Pubmed: Author and Title
Google Scholar: Author Only Title Only Author and Title

Bergmeyer HU, Bernt E (1974) Colorimetric Assay with l-Lactate, NAD Phenazine Methosulphate and INT. In HU Bergmeyer, ed, Methods of Enzymatic Analysis (Second Edition). Academic Press, pp 579-582

Pubmed: Author and Title
Google Scholar: Author Only Title Only Author and Title

Bienert GP, Desguin B, Chaumont F, Hols P (2013) Channel-mediated lactic acid transport: a novel function for aquaglyceroporins in bacteria. Biochem J 454: 559-570

Pubmed: Author and Title
Google Scholar: Author Only Title Only Author and Title

Boursiac Y, Prak S, Boudet J, Postaire O, Luu DT, Tournaire-Roux C, Santoni V, Maurel C (2008) The response of Arabidopsis root water transport to a challenging environment implicates reactive oxygen species- and phosphorylation-dependent internalization of aquaporins. Plant Signal Behav 3: 1096-1098

Pubmed: Author and Title
Google Scholar: Author Only Title Only Author and Title

Branco-Price C, Kaiser KA, Jang CJ, Larive CK, Bailey-Serres J (2008) Selective mRNA translation coordinates energetic and metabolic adjustments to cellular oxygen deprivation and reoxygenation in Arabidopsis thaliana. Plant J 56: 743-755

Pubmed: Author and Title
Google Scholar: Author Only Title Only Author and Title

Branco-Price C, Kawaguchi R, Ferreira RB, Bailey-Serres J (2005) Genome-wide analysis of transcript abundance and translation in Arabidopsis seedlings subjected to oxygen deprivation. Ann Bot 96: 647-660

Pubmed: Author and Title
Google Scholar: Author Only Title Only Author and Title

Chevalier AS, Chaumont F (2015) Trafficking of plant plasma membrane aquaporins: multiple regulation levels and complex sorting signals. Plant Cell Physiol 56: 819-829

Pubmed: Author and Title
Google Scholar: Author Only Title Only Author and Title

Choi WG, Roberts DM (2007) Arabidopsis NIP2;1, a major intrinsic protein transporter of lactic acid induced by anoxic stress. J Biol Chem 282: 24209-24218

Pubmed: Author and Title
Google Scholar: Author Only Title Only Author and Title

Clough SJ, Bent AF (1998) Floral dip: a simplified method for Agrobacterium-mediated transformation of Arabidopsis thaliana. Plant J 16: 735-743

Pubmed: Author and Title
Google Scholar: Author Only Title Only Author and Title

Collard F, Baldin F, Gerin I, Bolsee J, Noel G, Graff J, Veiga-da-Cunha M, Stroobant V, Vertommen D, Houddane A, Rider MH, Linster CL, Van Schaftingen E, Bommer GT (2016) A conserved phosphatase destroys toxic glycolytic side products in mammals and yeast. Nat Chem Biol 12: 601-607

Pubmed: Author and Title
Google Scholar: Author Only Title Only Author and Title

Counillon L, Bouret Y, Marchiq I, Pouyssegur J (2016) Na+/H+ antiporter (NHE1) and lactate/H+ symporters (MCTs) in pH homeostasis and cancer metabolism. Biochimica Et Biophysica Acta-Molecular Cell Research 1863: 2465-2480

Pubmed: Author and Title
Google Scholar: Author Only Title Only Author and Title

Davies DD, Grego S, Kenworthy P (1974) The control of the production of lactate and ethanol by higher plants. Planta 118: 297-310

Pubmed: Author and Title
Google Scholar: Author Only Title Only Author and Title

Dolferus R, Wolansky M, Carroll R, Miyashita Y, Ismond K, Good A (2008) Functional analysis of lactate dehydrogenase during hypoxic stress in Arabidopsis. Functional Plant Biology 35: 131-140

Pubmed: Author and Title
Google Scholar: Author Only Title Only Author and Title

Drew MC (1997) OXYGEN DEFICIENCY AND ROOT METABOLISM: Injury and Acclimation Under Hypoxia and Anoxia. Annu Rev Plant

Physiol Plant Mol Biol 48: 223-250
Pubmed: Author and Title
Google Scholar: Author Only Title Only Author and Title

Ellis MH, Dennis ES, Peacock WJ (1999) Arabidopsis roots and shoots have different mechanisms for hypoxic stress tolerance. Plant Physiol 119: 57-64
Pubmed: Author and Title
Google Scholar: Author Only Title Only Author and Title

Engqvist MK, Schmitz J, Gertzmann A, Florian A, Jaspert N, Arif M, Balazadeh S, Mueller-Roeber B, Fernie AR, Maurino VG (2015) GLYCOLATE OXIDASE3, a Glycolate Oxidase Homolog of Yeast l-Lactate Cytochrome c Oxidoreductase, Supports l-Lactate Oxidation in Roots of Arabidopsis. Plant Physiol 169: 1042-1061
Pubmed: Author and Title
Google Scholar: Author Only Title Only Author and Title

Faghiri Z, Camargo SM, Huggel K, Forster IC, Ndegwa D, Verrey F, Skelly PJ (2010) The tegument of the human parasitic worm Schistosoma mansoni as an excretory organ: the surface aquaporin SmAQP is a lactate transporter. PLoS One 5: e10451
Pubmed: Author and Title
Google Scholar: Author Only Title Only Author and Title

Felle HH (2005) pH regulation in anoxic plants. Annals of Botany 96: 519-532
Pubmed: Author and Title
Google Scholar: Author Only Title Only Author and Title

Gibbs J, Greenway H (2003) Mechanisms of anoxia tolerance in plants. I. Growth, survival and anaerobic catabolism (vol 30, pg 1, 1993). Functional Plant Biology 30: 353-U356
Pubmed: Author and Title
Google Scholar: Author Only Title Only Author and Title

Giuntoli B, Lee SC, Licausi F, Kosmacz M, Oosumi T, van Dongen JT, Bailey-Serres J, Perata P (2014) A trihelix DNA binding protein counterbalances hypoxia-responsive transcriptional activation in Arabidopsis. PLoS Biol 12: e1001950
Pubmed: Author and Title
Google Scholar: Author Only Title Only Author and Title

Greenway H, Gibbs J (2003) Mechanisms of anoxia tolerance in plants. II. Energy requirements for maintenance and energy distribution to essential processes. Functional Plant Biology 30: 999-1036
Pubmed: Author and Title
Google Scholar: Author Only Title Only Author and Title

Guenther JF, Chanmanivone N, Galetovic MP, Wallace IS, Cobb JA, Roberts DM (2003) Phosphorylation of soybean nodulin 26 on serine 262 enhances water permeability and is regulated developmentally and by osmotic signals. The Plant cell 15: 981-991
Pubmed: Author and Title
Google Scholar: Author Only Title Only Author and Title

Ishikawa F, Suga S, Uemura T, Sato MH, Maeshima M (2005) Novel type aquaporin SIPs are mainly localized to the ER membrane and show cell-specific expression in Arabidopsis thaliana. FEBS Lett 579: 5814-5820
Pubmed: Author and Title
Google Scholar: Author Only Title Only Author and Title

Ismond KP, Dolferus R, De Pauw M, Dennis ES, Good AG (2003) Enhanced low oxygen survival in Arabidopsis through increased metabolic flux in the fermentative pathway. Plant Physiology 132: 1292-1302
Pubmed: Author and Title
Google Scholar: Author Only Title Only Author and Title

Johanson U, Karlsson M, Johansson I, Gustavsson S, Sjovall S, Fraysse L, Weig AR, Kjellbom P (2001) The complete set of genes encoding major intrinsic proteins in Arabidopsis provides a framework for a new nomenclature for major intrinsic proteins in plants. Plant Physiol 126: 1358-1369
Pubmed: Author and Title
Google Scholar: Author Only Title Only Author and Title

Kamiya T, Fujiwara T (2009) Arabidopsis NIP1;1 transports antimonite and determines antimonite sensitivity. Plant Cell Physiol 50: 1977-1981
Pubmed: Author and Title
Google Scholar: Author Only Title Only Author and Title

Kamiya T, Tanaka M, Mitani N, Ma JF, Maeshima M, Fujiwara T (2009) NIP1;1, an aquaporin homolog, determines the arsenite sensitivity of Arabidopsis thaliana. J Biol Chem 284: 2114-2120
Pubmed: Author and Title
Google Scholar: Author Only Title Only Author and Title

Koncz C, Schell J (1986) The promoter of TL-DNA gene 5 controls the tissue-specific expression of chimaeric genes carried by a novel type of Agrobacterium binary vector. Molecular and General Genetics MGG 204: 383-396
Pubmed: Author and Title
Google Scholar: Author Only Title Only Author and Title

Kursteiner O, Dupuis I, Kuhlemeier C (2003) The pyruvate decarboxylase1 gene of Arabidopsis is required during anoxia but not other environmental stresses. Plant Physiol 132: 968-978
Pubmed: Author and Title
Google Scholar: Author Only Title Only Author and Title

Laemmli UK (1970) Cleavage of structural proteins during the assembly of the head of bacteriophage T4. Nature 227: 680-685
Pubmed: Author and Title
Google Scholar: Author Only Title Only Author and Title

Latham T, Mackay L, Sproul D, Karim M, Culley J, Harrison DJ, Hayward L, Langridge-Smith P, Gilbert N, Ramsahoye BH (2012) Lactate, a product of glycolytic metabolism, inhibits histone deacetylase activity and promotes changes in gene expression. Nucleic Acids Research 40: 4794-4803
Pubmed: Author and Title
Google Scholar: Author Only Title Only Author and Title

Lee SC, Mustroph A, Sasidharan R, Vashisht D, Pedersen O, Oosumi T, Voesenek LA, Bailey-Serres J (2011) Molecular characterization of the submergence response of the Arabidopsis thaliana ecotype Columbia. The New phytologist 190: 457-471
Pubmed: Author and Title
Google Scholar: Author Only Title Only Author and Title

Li X, Wang X, Yang Y, Li R, He Q, Fang X, Luu DT, Maurel C, Lin J (2011) Single-molecule analysis of PIP2;1 dynamics and partitioning reveals multiple modes of Arabidopsis plasma membrane aquaporin regulation. Plant Cell 23: 3780-3797
Pubmed: Author and Title
Google Scholar: Author Only Title Only Author and Title

Licausi F, van Dongen JT, Giuntoli B, Novi G, Santaniello A, Geigenberger P, Perata P (2010) HRE1 and HRE2, two hypoxia-inducible ethylene response factors, affect anaerobic responses in Arabidopsis thaliana. Plant J 62: 302-315
Pubmed: Author and Title
Google Scholar: Author Only Title Only Author and Title

Liu F, Vantoai T, Moy LP, Bock G, Linford LD, Quackenbush J (2005) Global transcription profiling reveals comprehensive insights into hypoxic response in Arabidopsis. Plant Physiol 137: 1115-1129
Pubmed: Author and Title
Google Scholar: Author Only Title Only Author and Title

Lokdarshi A, Conner WC, McClintock C, Li T, Roberts DM (2016) Arabidopsis CML38, a Calcium Sensor That Localizes to Ribonucleoprotein Complexes under Hypoxia Stress. Plant Physiol 170: 1046-1059
Pubmed: Author and Title
Google Scholar: Author Only Title Only Author and Title

Marbach EP, Weil MH (1967) Rapid enzymatic measurement of blood lactate and pyruvate. Use and significance of metaphosphoric acid as a common precipitant. Clin Chem 13: 314-325
Pubmed: Author and Title
Google Scholar: Author Only Title Only Author and Title

Mateluna P, Salvatierra A, Solis S, Nunez G, Pimentel P (2018) Involvement of aquaporin NIP1;1 in the contrasting tolerance response to root hypoxia in Prunus rootstocks. J Plant Physiol 228: 19-28
Pubmed: Author and Title
Google Scholar: Author Only Title Only Author and Title

Maurino VG, Engqvist MK (2015) 2-Hydroxy Acids in Plant Metabolism. Arabidopsis Book 13: e0182
Pubmed: Author and Title
Google Scholar: Author Only Title Only Author and Title

Mizutani M, Watanabe S, Nakagawa T, Maeshima M (2006) Aquaporin NIP2;1 is mainly localized to the ER membrane and shows root-specific accumulation in Arabidopsis thaliana. Plant and Cell Physiology 47: 1420-1426
Pubmed: Author and Title
Google Scholar: Author Only Title Only Author and Title

Murchie EH, Lawson T (2013) Chlorophyll fluorescence analysis: a guide to good practice and understanding some new applications. J Exp Bot 64: 3983-3998
Pubmed: Author and Title
Google Scholar: Author Only Title Only Author and Title

Mustroph A, Barding GA, Jr., Kaiser KA, Larive CK, Bailey-Serres J (2014) Characterization of distinct root and shoot responses to low-oxygen stress in Arabidopsis with a focus on primary C- and N-metabolism. Plant Cell Environ 37: 2366-2380
Pubmed: Author and Title
Google Scholar: Author Only Title Only Author and Title

Mustroph A, Lee SC, Oosumi T, Zanetti ME, Yang HJ, Ma K, Yaghoubi-Masihi A, Fukao T, Bailey-Serres J (2010) Cross-Kingdom Comparison of Transcriptomic Adjustments to Low-Oxygen Stress Highlights Conserved and Plant-Specific Responses. Plant Physiology 152: 1484-1500
Pubmed: Author and Title
Google Scholar: Author Only Title Only Author and Title

Mustroph A, Zanetti ME, Jang CJ, Holtan HE, Repetti PP, Galbraith DW, Girke T, Bailey-Serres J (2009) Profiling translatomes of discrete cell populations resolves altered cellular priorities during hypoxia in Arabidopsis. Proc Natl Acad Sci U S A 106: 18843-18848
Pubmed: Author and Title
Google Scholar: Author Only Title Only Author and Title

Niyikiza D, Piya S, Routray P, Miao L, Kim WS, Burch-Smith T, Gill T, Sams C, Arelli PR, Pantalone V, Krishnan HB, Hewezi T (2020) Interactions of gene expression, alternative splicing, and DNA methylation in determining nodule identity. Plant J
Pubmed: Author and Title
Google Scholar: Author Only Title Only Author and Title

Noda Y, Sasaki S (2006) Regulation of aquaporin-2 trafficking and its binding protein complex. Biochim Biophys Acta 1758: 1117-1125
Pubmed: Author and Title
Google Scholar: Author Only Title Only Author and Title

Pfaffl MW (2001) A new mathematical model for relative quantification in real-time RT-PCR. Nucleic Acids Res 29: e45
Pubmed: Author and Title
Google Scholar: Author Only Title Only Author and Title

Pommerrenig B, Diehn TA, Bernhardt N, Bienert MD, Mitani-Ueno N, Fuge J, Bieber A, Spitzer C, Brautigam A, Ma JF, Chaumont F, Bienert GP (2020) Functional evolution of nodulin 26-like intrinsic proteins: from bacterial arsenic detoxification to plant nutrient transport. New Phytol 225: 1383-1396
Pubmed: Author and Title
Google Scholar: Author Only Title Only Author and Title

Prak S, Hem S, Boudet J, Viennois G, Sommerer N, Rossignol M, Maurel C, Santoni V (2008) Multiple phosphorylations in the C-terminal tail of plant plasma membrane aquaporins: role in subcellular trafficking of AtPIP2;1 in response to salt stress. Mol Cell Proteomics 7: 1019-1030
Pubmed: Author and Title
Google Scholar: Author Only Title Only Author and Title

Ricoult C, Cliquet J-B, Limami AM (2005) Stimulation of alanine amino transferase (AlaAT) gene expression and alanine accumulation in embryo axis of the model legume Medicago truncatula contribute to anoxia stress tolerance. Physiologia Plantarum 123: 30-39
Pubmed: Author and Title
Google Scholar: Author Only Title Only Author and Title

Rivoal J, Hanson AD (1993) Evidence for a Large and Sustained Glycolytic Flux to Lactate in Anoxic Roots of Some Members of the Halophytic Genus Limonium. Plant Physiol 101: 553-560
Pubmed: Author and Title
Google Scholar: Author Only Title Only Author and Title

Roberts DM, Routray P (2017) The Nodulin26 Intrinsic Protein Subfamily. In F Chaumont, SD Tyerman, eds, Plant Aquaporins From Transport to Signaling. Springer International Publishing, pp 267-296
Pubmed: Author and Title
Google Scholar: Author Only Title Only Author and Title

Roberts JK, Callis J, Jardetzky O, Walbot V, Freeling M (1984) Cytoplasmic acidosis as a determinant of flooding intolerance in plants. Proc Natl Acad Sci U S A 81: 6029-6033
Pubmed: Author and Title
Google Scholar: Author Only Title Only Author and Title

Santoni V (2017) Plant Aquaporin Postranslational Regulation. In F Chaumont, SD Tyerman, eds, Plant Aquaporins From Transport to Signaling. Springer International Publishing, pp 83-105
Pubmed: Author and Title
Google Scholar: Author Only Title Only Author and Title

Sato T, Harada T, Ishizawa K (2002) Stimulation of glycolysis in anaerobic elongation of pondweed (Potamogeton distinctus) turions. J Exp Bot 53: 1847-1856
Pubmed: Author and Title
Google Scholar: Author Only Title Only Author and Title

Schneider CA, Rasband WS, Eliceiri KW (2012) NIH Image to ImageJ: 25 years of image analysis. Nat Methods 9: 671-675
Pubmed: Author and Title
Google Scholar: Author Only Title Only Author and Title

Silva AL, Dressano K, Ceciliato PHO, Guerrero-Abad JC, Moura DS (2018) Evaluation of Root pH Change Through Gel Containing pH-sensitive Indicator Bromocresol Purple. Bio-Protocol 8(7):e2796
Pubmed: Author and Title
Google Scholar: Author Only Title Only Author and Title

Sorenson R, Bailey-Serres J (2014) Selective mRNA sequestration by OLIGOURIDYLATE-BINDING PROTEIN 1 contributes to translational control during hypoxia in Arabidopsis. Proc Natl Acad Sci U S A 111: 2373-2378
Pubmed: Author and Title
Google Scholar: Author Only Title Only Author and Title

Sun SR, Li H, Chen JH, Qian Q (2017) Lactic Acid: No Longer an Inert and End-Product of Glycolysis. Physiology 32: 453-463

Pubmed: Author and Title
Google Scholar: Author Only Title Only Author and Title

Takano J, Miwa K, Fujiwara T (2008) Boron transport mechanisms: collaboration of channels and transporters. Trends Plant Sci 13: 451-457
Pubmed: Author and Title
Google Scholar: Author Only Title Only Author and Title

Takano J, Yoshinari A, Luu D-T (2017) Plant Aquaporin Trafficking. In F Chaumont, SD Tyerman, eds, Plant Aquaporins From Transport to Signaling. Springer International Publishing, pp 47-81
Pubmed: Author and Title
Google Scholar: Author Only Title Only Author and Title

Tsai KJ, Chou SJ, Shih MC (2014) Ethylene plays an essential role in the recovery of Arabidopsis during post-anaerobiosis reoxygenation. Plant Cell Environ 37: 2391-2405
Pubmed: Author and Title
Google Scholar: Author Only Title Only Author and Title

Vialaret J, Di Pietro M, Hem S, Maurel C, Rossignol M, Santoni V (2014) Phosphorylation dynamics of membrane proteins from Arabidopsis roots submitted to salt stress. Proteomics 14: 1058-1070
Pubmed: Author and Title
Google Scholar: Author Only Title Only Author and Title

Voesenek LA, Bailey-Serres J (2013) Flooding tolerance: O2 sensing and survival strategies. Curr Opin Plant Biol 16: 647-653
Pubmed: Author and Title
Google Scholar: Author Only Title Only Author and Title

Voesenek LA, Bailey-Serres J (2015) Flood adaptive traits and processes: an overview. New Phytol 206: 57-73
Pubmed: Author and Title
Google Scholar: Author Only Title Only Author and Title

Wallace IS, Choi WG, Roberts DM (2006) The structure, function and regulation of the nodulin 26-like intrinsic protein family of plant aquaglyceroporins. Biochim Biophys Acta 1758: 1165-1175
Pubmed: Author and Title
Google Scholar: Author Only Title Only Author and Title

Wang S, Yoshinari A, Shimada T, Hara-Nishimura I, Mitani-Ueno N, Feng Ma J, Naito S, Takano J (2017) Polar Localization of the NIP5;1 Boric Acid Channel Is Maintained by Endocytosis and Facilitates Boron Transport in Arabidopsis Roots. Plant Cell 29: 824-842
Pubmed: Author and Title
Google Scholar: Author Only Title Only Author and Title

Wang X, Fan C, Zhang X, Zhu J, Fu YF (2013) BioVector, a flexible system for gene specific-expression in plants. BMC Plant Biol 13: 198
Pubmed: Author and Title
Google Scholar: Author Only Title Only Author and Title

Weaver CD, Crombie B, Stacey G, Roberts DM (1991) Calcium-dependent phosphorylation of symbiosome membrane proteins from nitrogen-fixing soybean nodules : evidence for phosphorylation of nodulin-26. Plant Physiol 95: 222-227
Pubmed: Author and Title
Google Scholar: Author Only Title Only Author and Title

Woody ST, Austin-Phillips S, Amasino RM, Krysan PJ (2007) The WiscDsLox T-DNA collection: an arabidopsis community resource generated by using an improved high-throughput T-DNA sequencing pipeline. J Plant Res 120: 157-165
Pubmed: Author and Title
Google Scholar: Author Only Title Only Author and Title

Xia JH, Roberts J (1994) Improved Cytoplasmic pH Regulation, Increased Lactate Efflux, and Reduced Cytoplasmic Lactate Levels Are Biochemical Traits Expressed in Root Tips of Whole Maize Seedlings Acclimated to a Low-Oxygen Environment. Plant Physiol 105: 651-657
Pubmed: Author and Title
Google Scholar: Author Only Title Only Author and Title

Xia JH, Saglio PH (1992) Lactic Acid efflux as a mechanism of hypoxic acclimation of maize root tips to anoxia. Plant Physiol 100: 40-46
Pubmed: Author and Title
Google Scholar: Author Only Title Only Author and Title

Xu W, Dai W, Yan H, Li S, Shen H, Chen Y, Xu H, Sun Y, He Z, Ma M (2015) Arabidopsis NIP3;1 Plays an Important Role in Arsenic Uptake and Root-to-Shoot Translocation under Arsenite Stress Conditions. Mol Plant 8: 722-733
Pubmed: Author and Title
Google Scholar: Author Only Title Only Author and Title

Yeung E, Bailey-Serres J, Sasidharan R (2019) After The Deluge: Plant Revival Post-Flooding. Trends Plant Sci 24: 443-454
Pubmed: Author and Title
Google Scholar: Author Only Title Only Author and Title

Zhang D, Tang Z, Huang H, Zhou G, Cui C, Weng Y, Liu W, Kim S, Lee S, Perez-Neut M, Ding J, Czyz D, Hu R, Ye Z, He M, Zheng YG,

Shuman HA, Dai L, Ren B, Roeder RG, Becker L, Zhao Y (2019) Metabolic regulation of gene expression by histone lactylation. Nature 574: 575-580

Pubmed: Author and Title
Google Scholar: Author Only Title Only Author and Title